Thionated Squaraine Molecules as Heavy-Atom-Free Sensitizers in NIR Upconversion Systems

Sarah R. Pristash

A dissertation

submitted in partial fulfillment of the

requirements for the degree of

Doctor of Philosophy

University of Washington

2022

Reading Committee:

Cody Schlenker, Chair

Daniel Gamelin

Matthew Golder

Program Authorized to Offer Degree:

Chemistry

University of Washington

Abstract

Thionated Squaraine Molecules as Heavy-Atom-Free Sensitizers in NIR Upconversion Systems

Sarah R. Pristash

Chair of the Supervisory Committee:
Cody W. Schlenker
Department of Chemistry

Solar energy conversion has the largest energy potential of all accessible energy resources. However, it is important to consider that the extractable amount of power from a solar cell is limited by the maximum cell efficiency. According to the detail-balance limit outlined by Shockley and Queisser, the maximum theoretical power conversion efficiency of a conventional solar cell is 33%, largely due to spectral mismatch between the solar spectrum and the cell absorption profile. One strategy for mitigating the loss of subgap photons is photon upconversion, which is a photophysical process that converts photons of lower energy to photons of higher energy in a 2-to-1 efficiency ratio. Triplet-triplet annihilation photon upconversion is a mechanism of upconversion that shows great promise due to its low incident power density requirements and highly tunable excitation and emission wavelengths. However, the triplet sensitizers used in the TTA-UC scheme typically involve precious metal complexes to induce the

heavy atom effect for efficient intersystem crossing, which provides a costly scalability barrier to widespread adoption of these systems.

Work enclosed in this dissertation outlines a novel heavy-atom-free TTA-UC sensitizer in the form of a thionated squaraine molecule. Importantly, the thionation of the squaraine inverts the lowest energy singlet states of the molecule, opening a channel for intersystem crossing as expected via El-Sayed's rule. Spectroscopic characterization of the thiosquaraine triplet reveals intersystem crossing in the thionated molecule within 4.5 ps of excitation, resulting triplet lifetime of 20 μs. This lifetime is sufficiently long for the necessary triplet-triplet energy transfer process to occur. A proof-of-concept upconversion system using the thiosquaraine as sensitizer and rubrene as the emitter molecule demonstrated successful upconversion with a quenching constant on the order of the diffusion rate of molecules in solution.

Further exploration of the thiosquaraine sensitizer revealed that it is able to convert deep red excitation to upconverted emission across the visible range. The highest peak-to-peak emission margin achieved with the thiosquaraine sensitizer is 0.8 eV, a record upconversion energy shift (UES) for a heavy-atom-free system. The squaraine platform provides a tunable template for additional heavy-atom-free sensitizers with absorption in the application-relevant near-infrared regime, and we explore the trade-offs between lowering the energy gap and the resulting triplet yield with a first-principles analysis.

TABLE OF CONTENTS

LIST OF FIGURES

LIST OF TABLES

ACKNOWLEDGEMENTS

I first must thank my advisor, Prof. Cody Schlenker, for his guidance over the last five and a half years. Thank you for your enthusiasm, your endless well of scientific ideas, and your thoughtful advice for planning my future – I often needed the reminders to not be afraid of my own success! I have grown so much as a scientist under your advisement, and I am excited to be working with you in the future as we explore the impact of our work.

Thank you to my committee for their time and interest in my work. To Professor Munira Khalil, who also served on my general committee and who gave her time willingly despite being at the helm of our department as our new Chair. To Professor Daniel Gamelin, thank you for your advice and practicality as we explore the future impact of the project; your experience is invaluable. Thank you to Professor Matthew Golder whom I am excited to work with more in the future. And a final thank you to my GSR, Professor Daniel Schwartz, who I've had the privilege of working with both through my work as a DIRECT Fellow and as a Torrance Science Policy Fellow. I truly learned so much from you in such a short time and I really appreciate getting to share my science with you as well! I'd also like to thank my previous committee members, Professor Joshua Vaughn and Professor Vincent Holmberg.

I must give a million thanks to all the members of the Schlenker Lab, both past and present. Being a part of this group of people has been one of the most rewarding experiences of my life. I must give an extra special thank you to both Drs. Kathryn Corp and Emily Rabe for all of their mentorship in my first few years in the lab – you both truly taught me everything I know and also were such an important part of my support system. I hope you know how much I truly admire you both and how grateful I am to have had you as not just mentors but also friends. I also must thank

Emma Cave for coming along with me on the experience of becoming senior members of the lab, which has been bizarre! I so appreciate your friendship and our mutual love of dogs and memes. Thanks to all of my desk mates tucked in our little corner of the office with me, as I consistently distracted each one of you – Dr. Jarred Olson, Ryan Flores, and Mark Bertolami. Jarred, I am so thankful for your friendship and glad that we appreciate the same kind of silliness that made working next to each other so much fun. Ryan, I'm so glad you're back in Seattle and I know you'll continue to do great things. And Mark, you've been such a joy to mentor. I so appreciate your thoughtful approach to learning and also that we can talk about Drag Race together. To all our other current lab members – Doyk Hwang, Liam Wrigley, Tyson Carr, Cecily Rosenbaum, Alexis Glaudin, Chris Tran, Micah Lee, and Meghna Shankar – I am so happy to see that the lab is in excellent hands moving forward, and that our tradition of comaraderie will continue!

I need to thank my entire cohort of students entering the graduate program in 2016 – it was very daunting moving across the country to a place where I didn't know anyone, but being with this group of people made it feel like I was fully supported in that experience. I want to especially thank Dylan Rogers, Jacob Ziegler, and Nora Munger for being excellent trivia, board game, and pie-making friends. And of course, I must give the most wholehearted of thanks to Drs. Lizzy Canarie and Chantelle Leveille, who have been with me every step of the way in graduate school from our first problem sets in quantum mechanics to our graduations this year. You both supported me through every struggle and I couldn't have achieved this without you. We did it!! And Lizzy, who has taken care of me well beyond any academic trouble into any aspect of my life, whether that be driving me to my wisdom teeth surgery or giving me a place to stay when I lock myself out of the house. I love you so much.

Also thanks to all of the other friends I have made in Seattle, both within the graduate program and without. Thanks so much to Ashley Dostie – I'm so glad we found each other when we did and you've been such a great friend. To my Kate's crew – Kelsey, Eedann, and Danika, I value your friendship so much and you've really helped make Seattle feel like a home. To Trevor and Camille, thanks for including me on so many of your adventures and for being my neighbors for so long!

To my Rochester friends, thank you for your many years of friendship. To Paul, Anthony, and Brendan – thank you for celebrating the New Year every year with me in NYC, for coming out to visit, and for being my besties for all this time. Extra special thank you to Paul whose brain mine melds with like nobody else. To all the Hoeing boys – Joe, Wes, Aaron, Dan, and Nate – thank you for always being willing to discuss TV and movies with me, for the endless bits that keep me laughing, and for always being willing to hop on a Zoom hang – you've truly kept me sane over the last few years!

To my friends from Cortland – Caitlin B, Caitlin T, Katylyn A, Katie, and Alex – I don't know what I could ever say that would be enough to describe how much your friendship means to me. You guys are so much a part of me and who I am today. You're truly my family. Thank you for being there, thank you for loving me. An extra special squeeze of love to my Caitlins whom I can't wait to grow old in the retirement home with. You are my soul mates!

Last but certainly not least, I must thank my incredible family. To my brothers Brian and Teddy – I love you guys so much and you really are my very best friends. I'm so grateful to have grown up with you and no one else will ever understand me the way you two do. Brian, thank you so much for your pep talks – I don't think you realize how much strength I get from your belief in me. And Ted, thanks for always being my friend I can go to for a laugh or discussion of just about

anything. I'm so proud of the person you've grown up to be. And finally to my amazing parents, who have done everything in their power to make sure all of my dreams can come true, who have supported me through a career path they can't fully understand, and who I would be completely lost without.

DEDICATION

I dedicate this work to my wonderful and loving parents, Kevin and Teresa. Thanks for always believing there was nothing I couldn't do.

"What do we call visible light? We call it color. But the electromagnetic spectrum runs to zero in one direction and infinity in the other, so really, children, mathematically, all of light is invisible."

— Anthony Doerr, All the Light We Cannot See

Chapter 1. INTRODUCTION

1.1 HARNESSING THE FULL POTENTIAL OF SOLAR

Steadily increasing global energy demand continues to motivate interest in sustainable carbon-free energy sources. Solar energy is by far the most prevalent energy source. As such, solar photovoltaic (PV) technologies remain the platform of greatest promise for carbon-neutral energy generation. Traditional solar cell efficiencies are constrained by the detailed-balance limits outlined by Shockley & Queisser.[1] However, boosting efficiency, assuming trivial increases in module costs, continues to be one of the most compelling approaches to overcome the total balance of systems cost for solar PV installations. The majority of spectral losses in the Shockley-Queisser limit come from spectral mismatch, with photons higher than the materials' bandgap being thermalized and photons below the materials' bandgap being transmitted through the cell. These spectral losses account for 58% of the overall efficiency loss.[1] As such, addressing any component of this spectral mismatch could have a large impact on the efficiency of the cell. Photon upconversion (UC) has the practical potential to foster PV technologies that exceed the Shockley-Queisser limit, by increasing practical single-junction efficiencies limits from roughly 31% to 40%, when UC is paired with multiple-exciton generation.[2] UC processes use the portion of the solar photons that possess insufficient energy to excite electronic transitions above the semiconductor's bandgap energy, which would otherwise be transmitted through the solar cell, just as window glass transmits visible light but blocks UV light. These sub-gap photons are then converted into above-gap photons that can produce electrical photocurrent in the cell.[3-6] A commonly-explored strategy for achieving upconversion using incoherent solar photons involves combining the energy of two molecular chromophores in their

respective triplet spin multiplicity excited states, in a process known as triplet-triplet annihilation (TTA). TTA-UC also has potential applications in photocatalysis,[7-8] bioimaging,[9] and sensing and detection.[10] The conservative estimate given above for PV efficiencies up to 40% will require an UC efficiency of 25% for NIR sub-gap absorption, as outlined in an analysis by David Cahen analysis and illustrated in **Figure 1.1**.[2] While visible TTA-UC efficiencies exceeding 10% at one sun have been reported,[11] these systems utilize expensive sensitizers whose absorbance is within, and not outside, the response profile of commercial solar materials. Major scientific and technological strides toward scalable and stable NIR sub-gap UC sensitizers will be required to realize practical PV technologies capable of breaking the Shockley-Queisser limit. Herein, we propose a strategy of thionating carbonyl groups on common organic dyes to produce efficient heavy-atom-free sensitizer molecules, vastly improving the cost efficiency and thus the scalability of the TTA-UC process. Below we discuss a specific example wherein we successfully implemented this strategy using a thionated squaraine dye as a TTA-UC sensitizer.

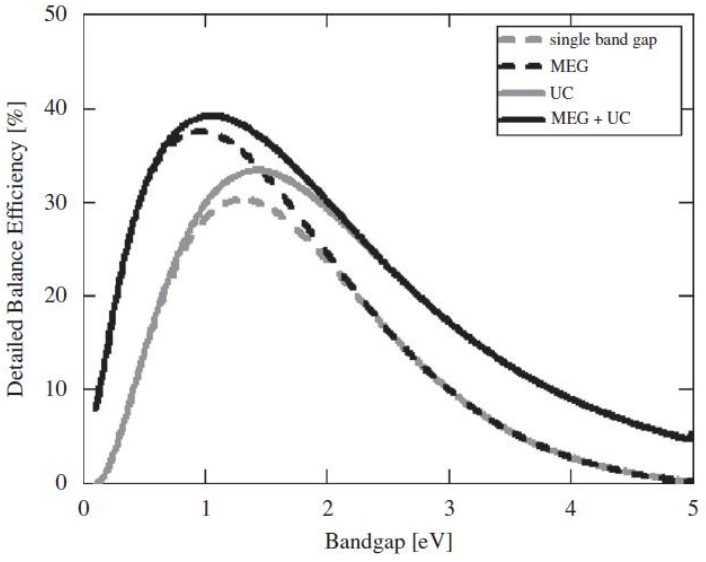

Figure 1.1. Detailed balance efficiency for a single bandgap solar cell as a function of band gap energy (dashed grey line). The efficiency enhancements given by multi-exciton generation (dashed black line), upconversion (solid grey line), or a combination of both technologies (solid black line) are also shown. Figure is reproduced from reference [2].

1.2 History of TTA-Upconversion

Of the several available strategies, photon upconversion by triplet-triplet annihilation (TTA) is particularly promising since it operates at comparatively low incident optical powers and under incoherent illumination. The mechanism for TTA-UC was first reported in the 1960s by Parker and Hatchard.[12] The mechanism they laid out will be described in a later section. As indicated by the name, TTA-UC is driven by triplet sensitization and thus requires molecules with high intersystem crossing (ISC) yields. In Parker and Hatchard's demonstration, however, both molecules had relatively low ISC yields, requiring low temperatures for the measurements, and the upconversion was relatively inefficient.[12] TTA-UC did not become popularized until decades later, when transition metal complexes were introduced to enhance the spin-orbit coupling and produce near-unity intersystem crossing yields of the sensitizer molecules.[13]

1.3 Thionated Organics for Fast Triplet Generation

Considering the TTA upconversion mechanism, certain characteristics are required in each molecule of the upconversion system. The sensitizer molecule must have a high triplet yield, a rapid intersystem crossing rate, and a triplet lifetime sufficiently long enough to facilitate TTET. The emitter molecules should have high fluorescence yields and practically forbidden intersystem crossing. Many polycyclic aromatic hydrocarbons meet the necessary requirements for emitter molecules in TTA upconversion systems, and thus organic molecules have been frequently employed as the fluorescent component of the system. However, it remains a challenge to design fully organic sensitizers for the TTA-UC process. This is notably because the relationship between electronic structure and intersystem crossing efficiency is multifaceted,

with few clear guiding molecular design principles for obtaining heavy-atom-free molecules with near-unity triplet yields *and* desirable absorption properties.[14] The best TTA-UC quantum efficiencies have historically been achieved using transition metal or organometallic triplet sensitizers, whose heavy atom metal centers induce large spin-orbit coupling constants. Many of these organometallic complexes rely on precious metal centers, such as Pt(II), Pd(II), Ir(III), or Ru(II).[13, 15-17] Their precious metals make these sensitizers costly and, in certain cases, toxic,[18] which are potential impediments to industry-scale adoption. Furthermore, these complexes typically rely on metal-to-ligand charge transfer (MLCT) excitations and other comparatively low-oscillator strength transitions that under-utilize the full potential of organic chromophores.[8, 19] Some success has been achieved in metal-free triplet sensitizers that incorporate heavy atoms, typically halogens, such as in the case of iodinated BODIPY-derivatives.[18] These organohalide bonds are photolabile and tend to limit the utility of these molecules as upconversion sensitizers.[18] To develop practical heavy-atom-free upconversion systems, it is compelling to identify new strategies for increasing the triplet yield of organic photosensitizers with intense absorption strength in the device-relevant NIR spectral region.

One strategy for developing all-organic, heavy-atom-free photosensitizers involves utilizing $n\pi^*$ states to enhance intersystem crossing to closely lying $\pi\pi^*$ triplet states,[20] as predicted by El-Sayed's Rules. Literature dating back as far as the 1970s[21] has shown that thionating pendant carbonyl groups on various aromatic core structures can open El Sayed-allowed intersystem crossing channels. This strategy has recently been applied to classes of molecules such as perylenediimides,[22] naphthalenediimides,[23] thymines,[24] perinones,[25] and, through our work, on squaraine dyes.[26] Given the facile synthesis and the wide range of accessible derivatives, this thionation approach appears to be a compelling path forward in develop organic, heavy-atom-

free sensitizers for TTA upconversion systems. However, several challenges remain in determining appropriate classes of molecules with which to utilize this strategy.

1.4 REFERENCES

1. Shockley, W.; Queisser, H. J., *J. Appl. Phys.* **1961,** *32*, 510-519.

2. Shpaisman, H.; Niitsoo, O.; Lubomirsky, I.; Cahen, D., *Sol. Energy Mater. Sol. Cells* **2008,** *92*, 1541-1546.

3. Frazer, L.; Gallaher, J. K.; Schmidt, T. W., *ACS Energy Lett.* **2017,** *2*, 1346-1354.

4. Schulze, T. F.; Czolk, J.; Cheng, Y.-Y.; Fückel, B.; MacQueen, R. W.; Khoury, T.; Crossley, M. J.; Stannowski, B.; Lips, K.; Lemmer, U.; Colsmann, A.; Schmidt, T. W., *J. Phys. Chem. C.* **2012,** *116*, 22794-22801.

5. Cheng, Y. Y.; Fückel, B.; MacQueen, R. W.; Khoury, T.; Clady, R. G. C. R.; Schulze, T. F.; Ekins-Daukes, N. J.; Crossley, M. J.; Stannowski, B.; Lips, K.; Schmidt, T. W., *Energy and Environmental Science* **2012,** *5*, 6953-6959.

6. Ha, S. J.; Kang, J. H.; Choi, D. H.; Nam, S. K.; Reichmanis, E.; Moon, J. H., *ACS Photonics* **2018,** *5*, 3621-3627.

7. Khnayzer, R. S.; Blumhoff, J.; Harrington, J. A.; Haefele, A.; Deng, F.; Castellano, F. N., *Chem. Comm.* **2012,** *48*, 209-211.

8. Islangulov, R. R.; Castellano, F. N., *Angew. Chem. Int. Ed.* **2006,** *45*, 5957-5959.

9. Liu, Q.; Xu, M.; Yang, T.; Tian, B.; Zhang, X.; Li, F., *ACS Appl. Mater. Interfaces* **2018,** *10*, 9883-9888.

10. Zhou, N.; Xu, B.; Gan, L.; Zhang, J. P.; Han, J. B.; Zhai, T. Y., *J. Mater. Chem. C.* **2017,** *5* (7), 1591-1595.

11. Hoseinkhani, S.; Tubino, R.; Meinardi, F.; Monguzzi, A., *Phys. Chem. Chem. Phys.* **2015,** *17*, 4020-4024.

12. Parker, C. A.; Hatchard, C. G., *Proceedings of the Chemical Society* **1962**, 386-387.

13. Singh-Rachford, T. N.; Castellano, F. N., *Coord. Chem. Rev.* **2010,** *254*, 2560-2573.

14. Zhao, J.; Chen, K.; Hou, Y.; Che, Y.; Liu, L.; Jia, D., *Org. Biomol. Chem.* **2018,** *16*, 3692-3701.

15. Cui, X.; Zhao, J.; Yang, P.; Sun, J., *Chem. Comm.* **2013,** *49*, 10221-10223.

16. Castellano, F. N.; Singh-Rachford, T. N., *J. Phys. Chem. A.* **2008,** *112* (16), 3550-3556.

17. Kimizuka, P. D.; Nobuhiro, Y.; Nobuo, *Chem. Comm.* **2014,** *50*, 13111-13113.

18. Wu, W.; Guo, H.; Wu, W.; Ji, S.; Zhao, J., *J. Org. Chem.* **2011,** *76*, 7056-7064.

19. Ji, S.; Guo, H.; Wu, W.; Wu, W.; Zhao, J., *Angew. Chem. Int. Ed.* **2011,** *50*, 8283-8286.

20. Castellano, T. N. S.-R.; Felix, N., *J. Phys. Chem. A.* **2009,** *113* (20), 5912-5917.

21. Anderson, R. W.; Hochstrasser, R. M.; Pownall, H. J., *Chemical Physics Letters* **1976,** *43*, 224-227.

22. Tilley, A. J.; Pensack, R. D.; Lee, T. S.; Djukic, B.; Scholes, G. D.; Seferos, D. S., *J. Phys. Chem. C.* **2014,** *118*, 9996-10004.

23. Hussain, M.; Zhao, J.; Yang, W.; Zhong, F.; Karatay, A.; Yaglioglu, H. G.; Yildiz, E. A.; Hayvali, M., *J. Lumin.* **2017,** *192*, 211-217.

24. Pollum, M.; Jockusch, S.; Crespo-Hernández, C. E., *J. Am. Chem. Soc.* **2014,** *136*, 17930-17933.

25. Palmer, J. R.; Wells, K. A.; Yarnell, J. E.; Favale, J. M.; Castellano, F. N., *The Journal of Physical Chemistry Letters* **2020,** *11*, 5092-5099.

26. Pristash, S. R.; Corp, K. L.; Rabe, E. J.; Schlenker, C. W., *ACS Applied Energy Materials* **2019**, acsaem.9b01808.

Chapter 2. BACKGROUND

2.1 Photoexcitation and Deactivation in Organic Molecules

When a molecule interacts with a photon of sufficient energy, an electronic transition can occur between electronic energy levels. Contained within these electronic energy levels are many vibrational energy levels that create a continuum of energies that can be absorbed by the molecule. Following photoexcitation, the molecule is in a non-equilibrium state and must relax back to its ground state. There are many different pathways of deactivation, and the relative prevalence of each deactivation pathway will depend on the rate constant of the transition. By Kasha's Rule,[1] vibrational relaxation to the lowest energy nuclear geometry happens much more quickly than electronic relaxation. Therefore, emission nearly always occurs from the lowest energy vibrational state within the manifold, resulting in an energetic shift between the absorption and the emission, known as the Stokes shift.[2] Whether or not emission occurs at all is dependent on the rate of radiative decay vs. non-radiative decay, i.e. the rate of fluorescence vs. that of internal conversion to a vibrational state of S_0.

An additional consideration is whether the electronic state is of singlet or triplet character. These electronic states are distinguished by the pairing of electron spins in the state. A singlet state has a single type of spin pairing – that of opposite or "up" and "down" spins. These states involve no transitions in the spin state and thus are strongly "allowed" and decay on the order of picoseconds to nanoseconds. A triplet state, however, involves a pairing that results in an overall net spin of one for the pair. Three electron pairings can result in such a spin value and are shown below in **Figure 2.1**.

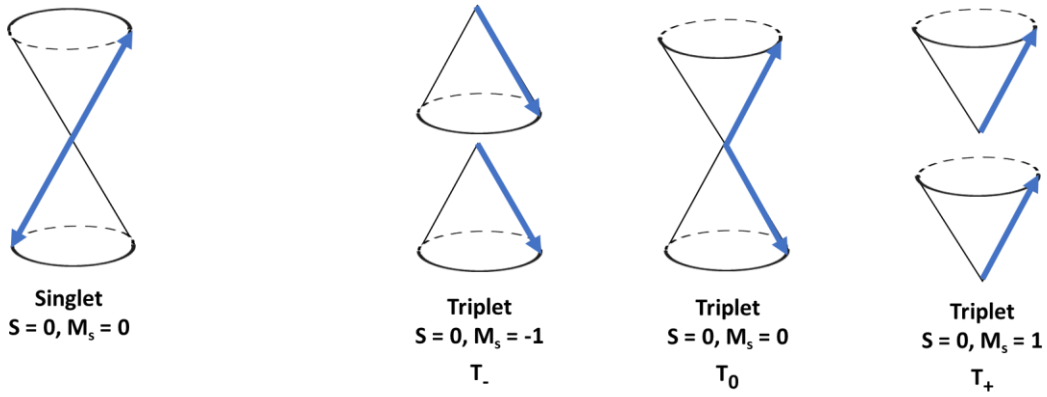

Figure 2.1. A spin diagram representing possible spin pairs to produce singlet and triplet electronic states.

The formation of a triplet state involves a flip in spin. This transition between the singlet and triplet manifold is known as intersystem crossing, which is classically forbidden and thus occurs on a much slower timescale. Intersystem crossing can be enhanced by coupling the change in spin to a change in orbital angular momentum, known as spin-orbit coupling. An emissive transition from the triplet state back to the singlet ground state is known as phosphorescence, which occurs on the timescale of nanoseconds to milliseconds. **Figure 2.2** depicts a Jablonski diagram, which pictorially represents the possible relaxation mechanisms of the molecule following photoexcitation. An excellent resource for a more in-depth discussion of molecular photophysical processes is Turro's *Modern Molecular Photochemistry.*[3]

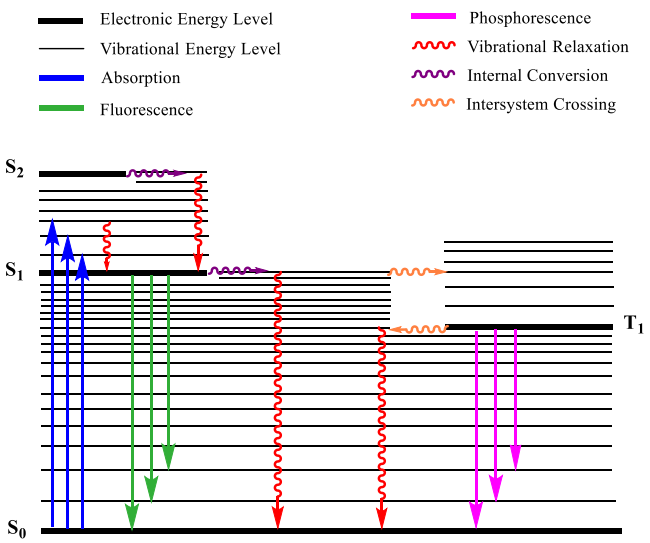

Figure 2.2. Jablonski diagram showing possible deactivation pathways for an organic molecule following absorption.

2.2 PHOTOPHYSICS OF TRIPLET-TRIPLET ANNIHILATION UPCONVERSION

The upconversion mechanism outlaid by Parker and Hatchard[4] in 1962 involves a series of energy transfer steps between two molecules. First, a sensitizer molecule is excited and undergoes intersystem crossing to its triplet state, after which Dexter or triplet-triplet energy transfer (TTET) occurs to the emitter molecule. Two emitter molecules with an appropriate combination of triplet excited states can then annihilate through an overall spin conserved process, leaving one in its singlet excited state and one in its singlet ground state. The singlet excited state radiatively relaxes, fluorescing at a higher energy than the incident absorbed photons. The wavelength of excitation and emission can thus be easily tuned through selection of the appropriate sensitizer/emitter combination and upconversion can be achieved without coherent excitation. This mechanism is displayed in **Figure 2.3**.

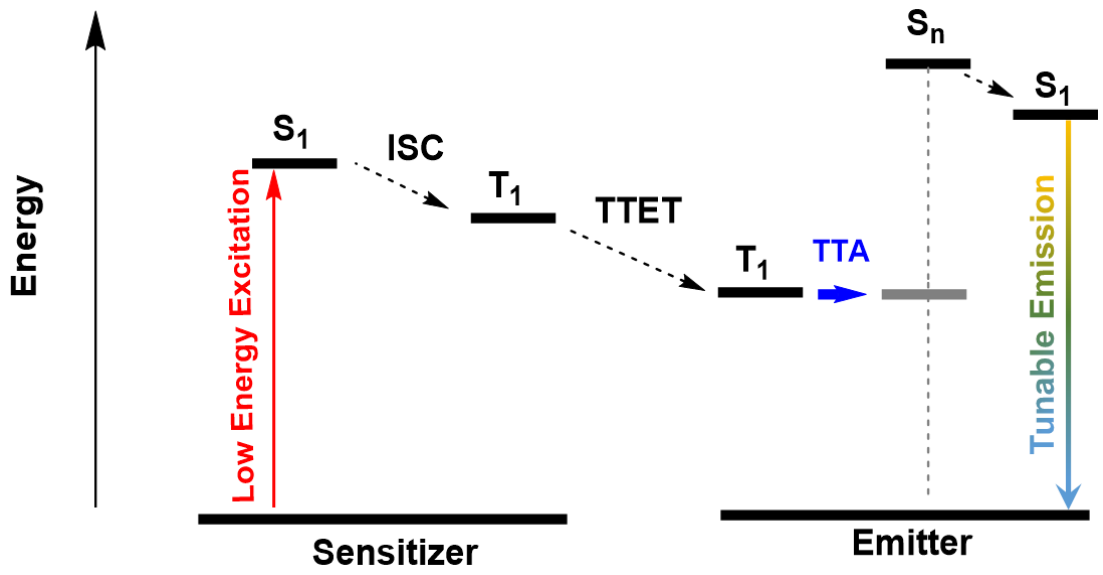

Figure 2.3. Triplet-tripet annihilation upconversion (TTA-UC) mechanism.

Upon the collision process of TTA, it is important to note that the generated exciton will have differing spin depending on the statistical combinations of the spins of the colliding triplets. In essence, the statistical distribution of colliding triplet pairs is shown below:

$$T_1 + T_1 \Rightarrow \begin{Bmatrix} Q + S_0 \text{ (multiplicity 5)} \\ T + S_0 \text{ (multiplicity 3)} \\ S + S_0 \text{ (multiplicity 1)} \end{Bmatrix}$$

Figure 2.4. Spin statistics of triplet pair combinations

Thus, from a purely spin-statistical perspective, it would appear that there is only a 1/9 chance of forming a radiative singlet state, or 11%. However, from a practical standpoint, the spin-statistical limit can be readily surpassed. First one can consider the formation of a quintet state as generally energetically inaccessible. Additionally, consider the formation of a triplet state from the triplet pair. As long as a sufficient population of triplets is maintained, the resulting triplet may undergo a second TTA process, allowing more opportunities for singlet formation. Finally,

if the emitter is energetically structured such that the T_2 energy is greater than that of $2T_1$, the triplet state also becomes energetically inaccessible, leading to the unity formation of singlets upon annihilation. This sort of spin-statistical consideration can be used to evaluate annihilators for their efficiency in a TTA-UC system.[5-6]

The triplet-triplet annihilation upconversion mechanism involves many energy transfer steps among various excited states, resulting in a significant number of characterization parameters for the system. For reference, a table of some common terms used in discussing TTA-UC is provided as **Table 2.1**.

Table 2.1 Common constants used in description of TTA-UC systems.

Term	Definition
k_{isc}	Intersystem crossing rate constant
τ_{isc}	Intersystem crossing time
k_{TTET}	Triplet-triplet energy transfer rate constant
k_q	Quenching rate constant
k_r	Rate constant of radiative decay
k_{nr}	Rate constant of non-radiative decay
Φ_{UC}	Upconversion quantum yield
Φ_T	Triplet generation yield
τ_T	Triplet lifetime
ε	Molar extinction coefficient

2.3 Lock-In Amplification

Measuring a small excited-state population with finite lifetime within a large bulk population of ground-state chromophores presents a challenge for studying excited states in organic molecules. To overcome a low signal-to-noise ratio, we use amplitude-modulated excitation and lock-in amplification. By modulating the source of photoexcitation (e.g., an LED or laser diode) we are able to selectively extract the resulting signals that show the same modulated frequency. Within this work, lock-in amplified detection is used for both photoinduced absorption (PIA) and photoluminescence (PL) measurements. A schematic diagram of the lock-in amplified spectroscopic set up is shown below as **Figure 2.5**.

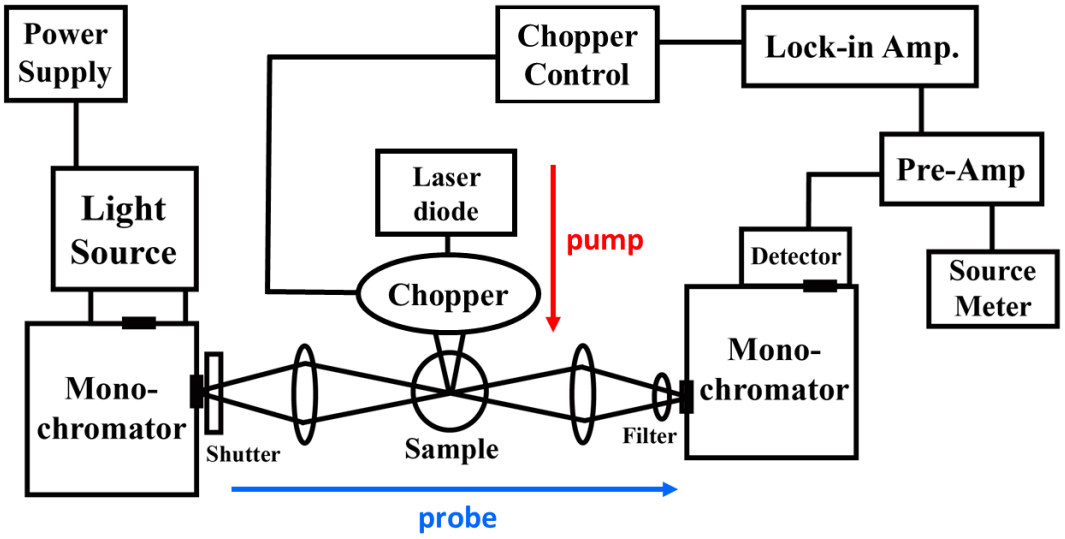

Figure 2.5. Schematic diagram of lock-in induced spectroscopic measurements set up.

In this schematic, the laser diode is used as a pump beam, which is mechanically modulated with a chopper. In photoinduced absorption measurements, a monochromated halogen lamp is used as the probe beam. Both beams are focused on the sample and either the probe or the luminescence is focused into a detector. The detector is passed to a lock in amplifier via a pre-amplifier. This

converts the generated photocurrent on the photodiode detector to a voltage and provides a small amount of initial amplification. The lock-in amplifier is referenced to the frequency of the pump beam, so only signal that modulates with the frequency of the pump is collected. A source meter also measures the steady signal on the detector to normalize spectra to the detector response. In the photoluminescence experiment, the setup is essentially the same, but as the probe beam is no longer needed, the pump acts independently and the collected signal at the detector is resulting from the luminescence of the sample.

2.4 Transient Absorption Spectroscopy

To gain additional kinetic information on the evolution of excited state spectra, a useful technique is transient absorption spectroscopy. Transient absorption is a pump-probe technique much like photoinduced absorption described above, but in this technique the probe is either electronically or mechanically delayed to arrive at discrete times after the pump pulse, allowing the kinetic evolution of the spectra to be monitored. A general schematic of the transient absorption setup is shown in **Figure 2.6**. Briefly, both a probe and pump pulse are generated and focused cospatially onto the sample. The probe beam is split to provide a reference, which accounts for spectral fluctuations and detector responses to the probe. Data is collected and plotted as the differential optical density $\Delta OD = \log10\ [I_0\ \text{sample}/I_{ex}\ \text{sample} \times I_{ex}\ \text{ref}/I_0\ \text{ref}]$, where I is the difference in intensity of the transmission of either the initial (ground state) or the excited state of the sample when the pump is on vs. off.

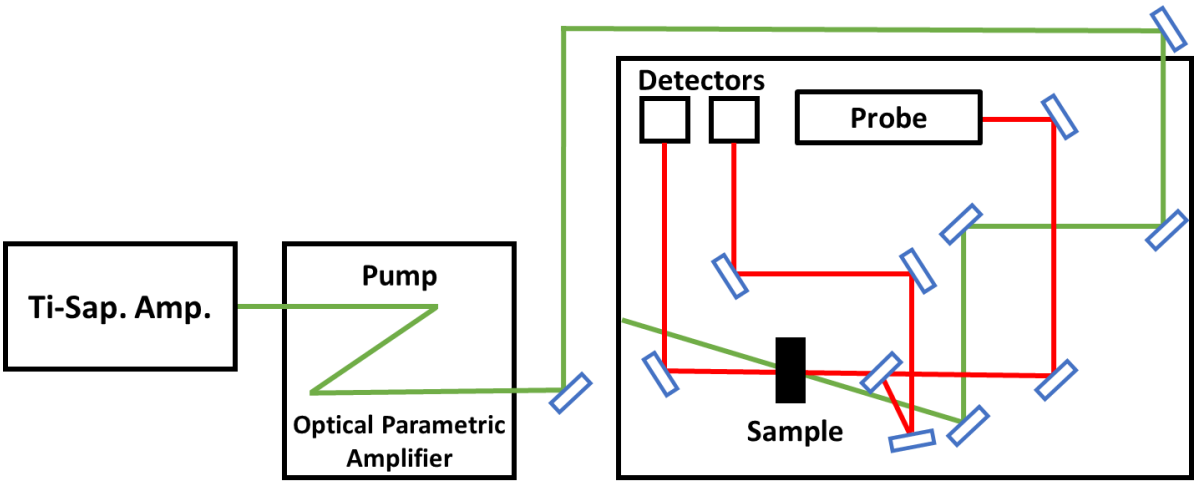

Figure 2.6. Schematic diagram of transient absorption setup.

2.5 TIME-RESOLVED PHOTOLUMINESCENCE

Much as transient absorption is a kinetically resolved analogue to steady-state photoinduced absorption, time-resolved photoluminescence serves to provide kinetic detail to photoluminescence measurement. As such, time-resolved photoluminescence allows for the measure of the rates of formation and decay of luminescent species. Time-resolved luminescence is helpful to determine how the various energy transfer steps of the upconversion process affect the luminescence kinetics.

In this work, two methods of time-resolved photoluminescence are used. The first is time-correlated single photon counting, or TCSPC. In the TCSPC measurement, a pulsed laser diode is used to excite a photoluminescence sample at a set repetition rate. The resulting photoluminescence is collected through a long-pass filter to remove any excitation light. The detector then detects a single luminescence photon after each pulse. This is repeated with each pulse, ultimately building a histogram of times at which a single photon arrives at the detector after the excitation pulse. This histogram can be fit to an exponential decay, resulting in a

luminescence lifetime. This method of measuring the PL lifetime has no spectral resolution, only resolution in time.

The second method of time-resolved photoluminescence used in this work is a streak camera. This method provides both spectral and temporal resolution and can measure on a wide range of timescales. In our setup, the sample is irradiated with ~50 fs pulses and the resulting photoluminescence is collected with a Hammatsu streak camera. After excitation with the pulsed laser, the orthogonal luminescence is spectrally resolved by focusing through a lens and dispersing onto a grating. The dispersed light then hits a photocathode which converts the emitted photons into electrons that then enter the streak tube. Within the streak tube, a voltage is triggered by the laser pulse. To provide the time resolution, the voltage is swept over time, which changes the path of the electron correspondingly. The electrons then hit a phosphor screen which converts them back into photons. A CCD camera images the resulting luminescence, giving an overall result with the vertical axis representing time and the horizontal axis representing wavelength.

2.6 Global Analysis

For all the time-resolved techniques discussed in this work, global analysis is a powerful tool to kinetically resolve overlapping spectral features. Global analysis does this by modeling the time- and wavelength-dependent spectrum as a function of both a time-dependent concentration $c_i(t)$ and a wavelength-dependent spectrum $\sigma_i(t)$, summed over the total species present. The resulting spectra are termed evalution-associated decay spectra, or EADS. To perform our gloabal analyses, our group uses GloTarAn, a graphical user interface for the R-package TIMP.[7]

2.7 REFERENCES

1. Kasha, M., **1950,** *9*, 14-19.

2. Stokes, G. G., **1852,** *142*, 463-562.

3. Turro, N. J.; Ramamurthy, V.; Scaiano, J. C., *Principles of Molecular Photochemistry: An Introduction*. University Science Books: Sausalito, California, 2009.

4. Parker, C. A.; Hatchard, C. G., *Proceedings of the Chemical Society* **1962**, 386-387.

5. Schmidt, T. W.; Castellano, F. N., *J. Phys. Chem. Lett.* **2014,** *5*, 4062-4072.

6. Cheng, Y. Y.; Fükel, B.; Khoury, T.; Clady, R. G. C. R.; Tayebjee, M. J. Y.; Ekins-Daukes, N. J.; Crossley, M. J.; Schmidt, T. W., **2010,** *1*, 1795-1799.

7. Snellenburg, J. J.; Laptenok, S. P.; Seger, R.; Mullen, K. M.; Stokkum, I. H. M. v., *J. Stat. Soft.* **2012,** *49*, 1-22.

Chapter 3. Synthesis, Quantum Chemical Analysis, and Design of Squaraine Molecules and their Thionated Analogues

This chapter will present the synthesis procedure for squaraine molecules and their thionated analogues, as well as a discussion of the energetic landscape of the squaraines and how it changes upon thionation. The trends observed in this study will be used to inform design of future squaraine derivatives, which is ongoing work in the Schlenker group.

3.1 Introduction to Squaraines

Squaraine are a class of organic, highly fluorescent, cyanine-type dyes, typically absorbing in the red or near infrared regions.[1-3] The squaraine structure is characterized by a highly electron-deficient aromatic four-membered ring at the core of the molecule.[4] The core is flanked with electron donating groups, often some sort of arylamine, resulting in an overall donor-acceptor-donor structure. Squaraines have been heavily studied in the fields of organic electronics,[3-7] biological imaging,[3] and photodynamic therapy.[1, 8]

3.2 Synthesis of Squaraines and Thiosquaraines

The squaraine synthesis has been reported as far back as 1966.[9] For symmetrical squaraines, the reaction involves the condensation of squaric acid with an arylamine or other electron-rich substituents via electrophilic aromatic substitution.

Synthesis of butylaniline squaraine: For the butylaniline squaraine derivative studied in this work, the reaction procedure is as follows[2]: squaric acid and dibutylaniline were combined in a round-bottomed flask equipped with a Dean−Stark apparatus. The mixture was dissolved in 50 mL of 1:1 toluene/N-butanol, then stirred under reflux for 5 h. The solvent was removed, and the

crude material was purified by column chromatography on silica gel, using a 2% EtOAC:Toluene mixture. The final structure was confirmed by ^{1}H NMR. A schematic of the butylaniline squaraine synthesis is show in **Figure 3.1**.

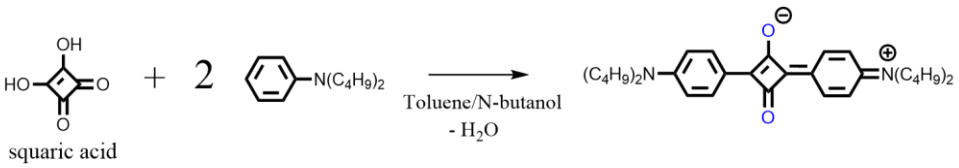

Figure 3.1. Schematic representation of the butylaniline squaraine synthesis.

Synthesis of thionated butylaniline squaraine (TSQ): To thionate the butylaniline squaraine, the squaraine was mixed with Lawesson's reagent in a 0.7:1 mol ratio[2]. The mixture was dissolved in toluene in an argon glovebox and stirred at room temperature for 30 min, over which time the color of the solution changed from blue to green. The crude product was purified by column chromatography on silica gel. The structure was confirmed via ^{1}H NMR. This thionated butylaniline squaraine is denoted as thiosquaraine or TSQ in this text. A schematic of the thionation procedure is shown in **Figure 3.2**.

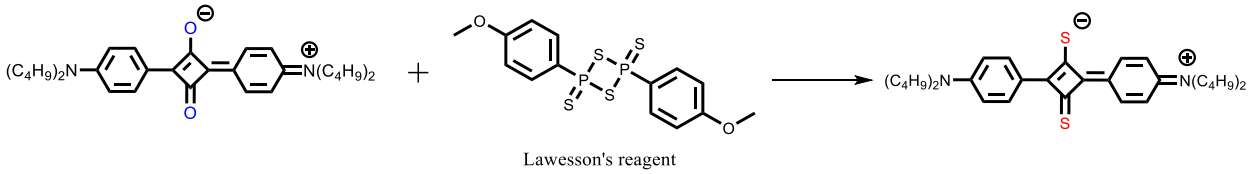

Figure 3.2. Schematic representation of the thionation procedure.

3.3 Effect of Thionation on the Squaraine Electronic Structure

The parent butylaniline squaraine derivative is, as is typical of squaraine molecules, highly fluorescent with a near-unity quantum yield.[8] Upon thionation, no fluorescence is observed due to a near-unity intersystem crossing yield to the triplet state. The triplet state is confirmed with

excited state absorption spectroscopies, as will be discussed in later chapters. Insight into this enhanced intersystem crossing in the thionated analogues can be found through molecular orbital calculations of the molecule.

The optimized geometries and electronic structures were calculated using time-dependent density functional theory through the Gaussian 16 suite of programs.[10] The B3LYP functional[11] was used with the 631G* basis set.[12] The solvation model density parameterization[13] function was used to simulate the effects of toluene. The resulting molecular orbital diagrams and leading singlet and triplet configurations are shown in **Table 3.1** and **Table 3.2**, respectively.

Table 3.1 Molecular orbital diagrams of butylaniline squaraine vs. thiosquaraine

	Squaraine	**Thiosquaraine**
LUMO	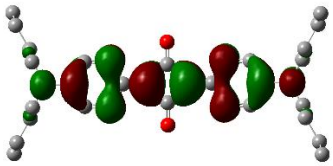	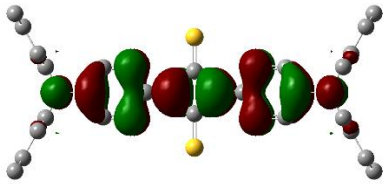
HOMO	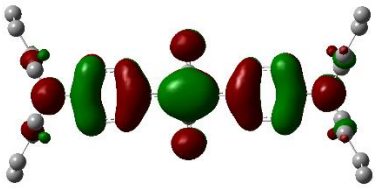	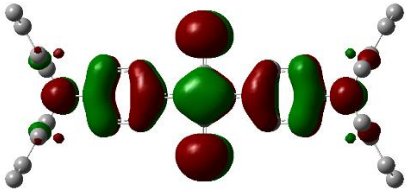
HOMO-1	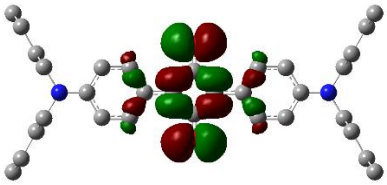	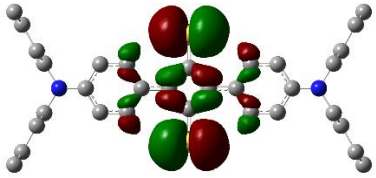

Table 3.2 Leading singlet and triplet configurations for selected energy states, squaraine and thiosquaraine[8]

	Squaraine – Leading configuration	**Thiosquaraine – Leading configuration**
S_1	HOMO → LUMO	HOMO-1 → LUMO
S_2	HOMO-2 → LUMO	HOMO → LUMO
T_1	HOMO → LUMO	HOMO → LUMO

As can be seen from **Table 3.1** and **Table 3.2**, the main difference in the energy manifolds between the squaraine and the thiosquaraine is the inversion of the two lowest lying singlet states. In the squaraine, the lowest lying singlet state is the HOMO → LUMO transition, which is of π-π* nature (**Table 3.1**). In contrast, when thionated, the lowest energy transition is now the HOMO-1 → LUMO transition. The HOMO-1 state is dominated by the nonbonding lone pairs on the sulfur atom, making this transition n-π* in nature. It is hypothesized that this singlet state inversion enhances the intersystem crossing rate in the thiosquaraine molecule because the rate of intersystem crossing is enhanced by the change in molecular orbital type, known as El-Sayed's rule.[14]

3.4 REFERENCES

1. Pristash, S. R.; Corp, K. L.; Rabe, E. J.; Schlenker, C. W., *ACS Applied Energy Materials* **2019**, acsaem.9b01808.

2. Webster, S.; Peceli, D.; Hu, H.; Padilha, L. A.; Przhonska, O. V.; Masunov, A. E.; Gerasov, A. O.; Kachkovski, A. D.; Slominsky, Y. L.; Tolmachev, A. I.; Kurdyukov, V. V.; Viniychuk, O. O.; Barrasso, E.; Lepkowicz, R.; Hagan, D. J.; Van Stryland, E. W., *J. Phys. Chem. Lett.* **2010,** *1*, 2354-2360.

3. He, J.; Jin Jo, Y.; Sun, X.; Qiao, W.; Ok, J.; Kim, T.-i.; Li, A.; He, J.; Sun, X.; Qiao, W.; Li, Z.; Jo, Y. J.; Ok, J.; Kim, T.-I., **2021,** *31*, 2008201.

4. Xia, G.; Wang, H., **2017,** *31*, 84-113.

5. Chen, G.; Sasabe, H.; Igarashi, T.; Hong, Z.; Kido, J., **2015,** *3*, 14517-14534.

6. Strassel, K.; Kaiser, A.; Jenatsch, S.; Véron, A. C.; Anantharaman, S. B.; Hack, E.; Diethelm, M.; Nüesch, F.; Aderne, R.; Legnani, C.; Yakunin, S.; Cremona, M.; Hany, R., *ACS Appl. Mater. Interfaces* **2018,** *10*, 11063-11069.

7. Ilina, K.; MacCuaig, W. M.; Laramie, M.; Jeouty, J. N.; McNally, L. R.; Henary, M., **2019,** *31*, 194-213.

8. Peceli, D.; Hu, H.; Fishman, D. A.; Webster, S.; Przhonska, O. V.; Kurdyukov, V. V.; Slominsky, Y. L.; Tolmachev, A. I.; Kachkovski, A. D.; Gerasov, A. O.; Masunov, A. E.; Hagan, D. J.; Van Stryland, E. W., *J. Phys. Chem. A.* **2013,** *117*, 2333-2346.

9. Sprenger, H. E.; Ziegenbein, W., **1966,** *5*, 894-894.

10. Frisch, M. J.; Trucks, G. W.; Schlegel, H. B.; Scuseria, G. E.; Robb, M. A.; Cheeseman, J. R.; Scalmani, G.; Barone, V.; Petersson, G. A.; Nakatsuji, H.; Li, X.; Caricato, M.; Marenich, A. V.; Bloino, J.; Janesko, B. G.; Gomperts, R.; Mennucci, B.; Hratchian, H. P.; Ortiz, J. V.; Izmaylov, A. F.; Sonnenberg, J. L.; Williams; Ding, F.; Lipparini, F.; Egidi, F.; Goings, J.; Peng, B.; Petrone, A.; Henderson, T.; Ranasinghe, D.; Zakrzewski, V. G.; Gao, J.; Rega, N.; Zheng, G.; Liang, W.; Hada, M.; Ehara, M.; Toyota, K.; Fukuda, R.; Hasegawa, J.; Ishida, M.; Nakajima, T.; Honda, Y.; Kitao, O.; Nakai, H.; Vreven, T.; Throssell, K.; Montgomery Jr., J. A.; Peralta, J. E.; Ogliaro, F.; Bearpark, M. J.; Heyd, J. J.; Brothers, E. N.; Kudin, K. N.; Staroverov, V. N.; Keith, T. A.; Kobayashi, R.; Normand, J.; Raghavachari, K.; Rendell, A. P.; Burant, J. C.; Iyengar, S. S.; Tomasi, J.; Cossi, M.; Millam, J. M.; Klene, M.; Adamo, C.; Cammi, R.; Ochterski, J. W.; Martin, R. L.; Morokuma, K.; Farkas, O.; Foresman, J. B.; Fox, D. J. *Gaussian 16 Rev. C.01*, Wallingford, CT, 2016.

11. Becke, A. D., **1998**.

12. Windus, V. A. R.; John, A. P.; Mark, A. R.; Theresa, L., **1998**.

13. Truhlar, A. V. M.; Christopher, J. C.; Donald, G., **2009**.

14. El-Sayed, M. A., *J. Chem. Phys.* **1963,** *38*, 2834-2838.

Chapter 4. Heavy-Atom-Free Red-to-Yellow Photon Upconversion

4.1 INTRODUCTION

As we continue in our search for carbon-neutral renewable energy sources, solar photovoltaics remain the platform of greatest promise for meeting ever-increasing global demand. However, traditional solar cell efficiencies are inherently capped at the detailed balance limit outlined by Shockley & Queisser.[1] This limit assumes that all incident sub-gap photons are transmitted, all above-gap photons generate carriers that thermalize to the semiconductor band edge, and all recombination losses occur radiatively. One potentially feasible strategy for possibly exceeding the Shockley-Queisser limit involves utilizing the sub-gap photons, which would otherwise be transmitted through the cell, by converting them into above-gap photons in a process known as photon upconversion.[2-3] Photon upconversion can be achieved in a series of photophysical steps that generate high-energy photons through sequential absorption of multiple quanta of low energy light. Upconversion has attracted research interest in recent years for applications in photovoltaics,[2-5] as well as photocatalysis,[6-7] sensing and detection,[8] and bioimaging.[9]

Triplet-triplet annihilation (TTA) photon upconversion is a particularly attractive upconversion mechanism for light-harvesting applications due to its relatively low incident optical power requirements, i.e., it can be achieved with the non-coherent light from solar illumination. In the TTA upconversion mechanism, a sensitizer molecule absorbs a low-energy photon, which results in a singlet excitation on the chromophore, which subsequently undergoes intersystem crossing to form a triplet excited state. Triplet-triplet energy transfer (TTET) then

occurs to an emitter molecule. Two emitter triplets can then annihilate via an overall spin-allowed electron exchange process to produce one emitter molecule in a singlet excited state and one emitter molecule in its singlet ground state. The singlet excited state radiatively relaxes, fluorescing at a higher energy than the incident absorbed photons (**Figure 2.3**). The wavelength of excitation and emission can thus be easily tuned by selecting an appropriate sensitizer/emitter combination.

Currently, the best TTA upconversion quantum efficiencies are achieved using transition metal or organometallic triplet sensitizers, wherein a heavy atom, typically a metal center, is required to induce large spin-orbit coupling constants. These organometallic complexes overwhelmingly rely on precious metals, such as Pt(II), Pd(II), Ir(III), or Ru(II).[10-13] However, employing precious metals makes sensitizers costly, which may present a significant scalability barrier for widespread adoption in solar upconversion systems. This is particularly true if one contemplates utilizing a platinum sensitizer, for example, on the scale of hundreds of thousands of square kilometers. In many cases these complexes also rely on low-energy MLCT and porphyrin Q-band excitations with fairly weak extinction coefficients,[7, 14-15] which implies that excess material is required for maximum photon absorption at longer wavelengths. Finally, the influence of the heavy atom effect, in terms of its spin-orbit coupling interaction, has been observed to diminish with increasing conjugation length in precious metal complexes.[16] Therefore, the efficiency of intersystem crossing is expected to diminish when extending the length of the chromophore's π-electron system to harvest sub-gap near-infrared (NIR) photons.

Considering the potential scalability challenges faced by light-harvesting upconversion systems that rely on precious metal centers, it is compelling to examine alternative molecular motifs. Organic sensitizers have the potential to be a comparatively lower-cost alternative to

precious metal complexes, while maintaining facile synthesis and purification routes. Some success has been achieved in avoiding precious metals by using iodinated and brominated dyes, boron dipyrromethene, or "BODIPY," derivatives are common examples.[17] However, introducing halogens as heavy-atom sensitizers carries the common unintended consequence of decreasing the photostability of the sensitizer due to photolysis reactions associated with the arylhalide. For example, multiple iodo-BODIPY-derivatives have been shown to begin photobleaching over a period of a few hours of illumination.[17] Despite this issue, there remain few examples of heavy atom-free organic upconversion sensitizers that avoid photoreactive halogens as a means of inducing intersystem crossing. There are reports of all-organic triplet sensitizers that operate through thermally activated delayed fluorescence, although these molecules typically have shorter triplet lifetimes that limit their energy transfer efficiencies.[18-19] A handful of all-organic sensitizers exist that utilize nπ states to enhance intersystem crossing to closely-lying ππ triplet states,[20] albeit usually with low extinction coefficients. The relationship between molecular structure and intersystem crossing efficiency for such all-organic chromophores comprises multiple factors, and it remains challenging to rationally design strongly-absorbing dyes that can act as efficient triplet sensitizers without incorporating heavy atoms.[21-22]

Herein, we present a metal-free and, indeed, entirely heavy atom-free TTA upconversion system, utilizing a strongly-absorbing thionated squaraine dye as the triplet sensitizer to convert low-energy red photons to higher-energy yellow photons. This heavy atom-free upconversion system is capable of operating under filtered non-coherent, simulated solar illumination. Both squaraines are synthesized through simple, single-step reactions, illustrated in Scheme 1. Importantly, incorporating sulfur into the squaraine core introduces non-bonding orbitals that

invert the native ordering of the $\pi\pi^*(S_1)$ and $n\pi^*(S_2)$ energy levels in the singlet landscape,[23-24] opening a channel for efficient intersystem crossing to the triplet state, as predicted by El Sayed's Rule, without relying on the heavy atom effect. The triplet state of the thiosquaraine is readily quenched by introducing rubrene in deaerated toluene solution, suggesting efficient triplet-triplet energy transfer, a key step to photon upconversion. For solar photovoltaic applications, upconversion systems that can be processed as thin-film solid-state coatings[25-28] are desirable for device integration. As such, we have also applied our thiosquaraine sensitizer to demonstrate photon upconversion from this system in a thin-film composite architecture.

4.2 Results and Discussion

The sensitizer, 2-(4-(Dibutylamino)phenyl)-4-(4-(dibutyliminio)cyclohexa-2,5-dien-1-ylidene)-3-thioxocyclobut-1-enethiolate, which we will refer to herein as thiosquaraine or TSQ, exhibits an intense absorption band (1.57×10^5 M^{-1} cm^{-1})[23] in the red portion of the visible spectrum, seen in **Figure 4.1**. The absorbance maximum is red-shifted from 636 nm in the parent squaraine to 685 nm upon thionation. Introducing sulfur non-bonding (n) orbitals inverts the native energy ordering of the $\pi\pi^*(S_1)$ and $n\pi^*(S_2)$ singlet transitions on the squaraine core (**Table 3.1**) and diminishes the lowest energy singlet-triplet energy splitting. As expected based on El-Sayed's Rule,[23, 29] these effects open a channel for efficient intersystem crossing in the thiosquaraine, without relying on the heavy atom effect. Evidence for this enhanced intersystem crossing is apparent in the lack of fluorescence at room temperature from TSQ, in contrast to a fluorescence quantum yield of $\Phi_f = 0.90$ that we measure for the unthionated parent squaraine. Fluorescence of the thiosquaraine is observed at 80K and is shown in **Figure A-4**. The structures of the parent and thionated squaraines are also displayed in **Figure 4.1**.

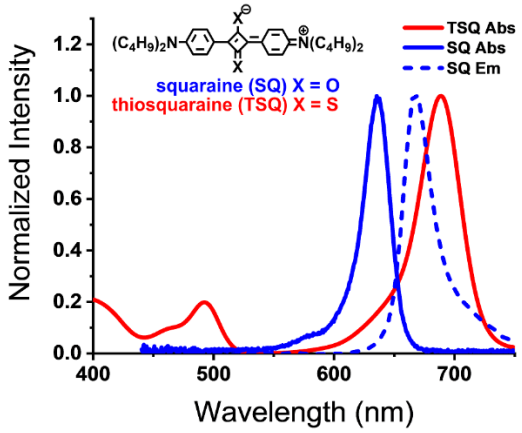

Figure 4.1. Absorbance (solid lines) characteristics of the parent squaraine (SQ) and thiosquaraine (TSQ) and room-temperature emission profile of SQ (dashed line) in toluene. We observe no room-temperature emission from TSQ. The chemical structures of the squaraines are displayed in the inset.

Photoinduced absorption (PIA) spectroscopy is a quasi-steady-state pump-probe photomodulation spectroscopy that monitors the differential transmission (ΔT) of a sample due to absorbance from long-lived, generally μs to ms, photoinduced excited-states, such as triplets and meta-stable charged species. When plotted relative to the sample's total optical transmission (T) at a given probe wavelength (λ), the normalized negative differential transmittance $-(\Delta T/T)$ is roughly equivalent to the differential absorption that is induced by the pump beam. Positive values for the quantity $-(\Delta T/T)$ correspond to photoinduced absorption features, while negative $-(\Delta T/T)$ values correspond to increases in transmission, or photoinduced bleaching. PIA measurements of the thiosquaraine in degassed toluene show an induced absorption band near 590 nm (**Figure 4.2**), which is consistent with previous reports of the thiosquaraine T_1-T_n photoinduced absorption,[23-24] and a characteristic negative peak corresponding to bleaching of the singlet ground state absorption at probe wavelengths near 685 nm. The 590 nm PIA and the concomitant bleach signal are both quenched in aerobic environments. This quenching is

presumably due to the sensitization of singlet oxygen, since thiosquaraine has been previously reported to catalyze oxygen luminescence,[24] indicating relatively efficient triplet formation on the thionated chromophore. We were unable to observe any thiosquaraine phosphorescence, even in the presence of ethyl iodide (an external heavy atom source) at low temperature. Phosphorescence would afford us a quantitative measure of the TSQ T_1 triplet energy. However, the singlet oxygen sensitization behavior of the molecule suggests that the triplet energy is above 1 eV.

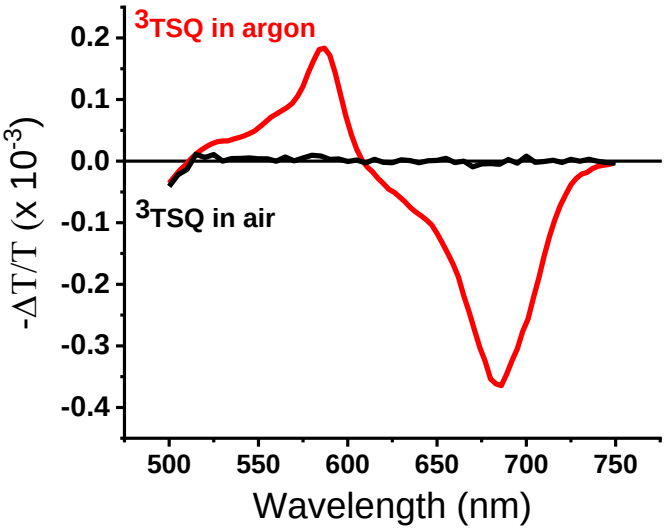

Figure 4.2. Quasi-steady-state photoinduced absorption (PIA) spectra of thiosquaraine in toluene. Under anaerobic conditions (red, ^{3}TSQ in argon) there is a strong $T_1 - T_n$ absorption at $\lambda_{probe} \sim 590$ nm and a corresponding $S_0 - S_1$ bleaching signature at $\lambda_{probe} \sim 685$ nm. These features are significantly quenched in aerobic conditions (black, ^{3}TSQ in air).

Because our PIA results indicated the thiosquaraine triplet was quenched by oxygen, we selected rubrene as a model emitter molecule for our upconversion system (**Figure 4.3**). Rubrene is a polycyclic aromatic hydrocarbon that has a triplet energy of $T_1 = 1.12$ eV and a Φ_f value that is near unity in solution. These properties make rubrene a frequent choice for NIR-to-visible upconversion schemes. The ground-state absorption and emission spectra for rubrene are shown

in **Figure 4.3**, overlaid with the thiosquaraine ground-state absorption for reference. The absorbance of rubrene exhibits a peak near 525 nm, which is sufficiently spectrally distinct from the TSQ absorption to allow us to selective excited the two chromophores independently. Perhaps more importantly, the rubrene fluorescence, which is represented by the dashed black trace in **Figure 4.3**, exhibits only a slight spectral overlap in the region between 600 – 675 nm with the TSQ absorption band. Minimizing this spectral overlap is important to help curtail parasitic Förster energy transfer back to the TSQ chromophore from the rubrene singlet excited state produced by upconversion.

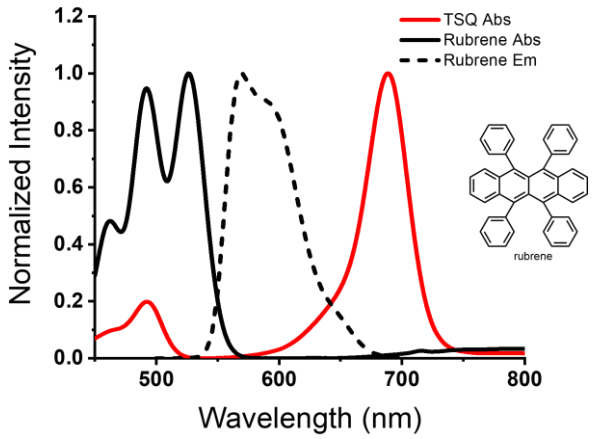

Figure 4.3. Absorption (solid black line) and emission (dashed black line) characteristics of rubrene compared to the thiosquaraine absorption spectrum (solid red line).

Selectively exciting the thiosquaraine molecule in the presence of rubrene results in upconverted fluorescence that is spectrally indistinguishable from the native rubrene singlet emission (**Figure 4.4a**, λ_{ex} = 685 nm). The anti-Stokes shift is 0.37 eV between the excitation wavelength and emission peak. For the excitation levels used in this study, we observe no room-temperature fluorescence from either component when they are pumped at 685 nm in isolation from the complementary upconversion component. This is seen in **Figure 4.4a**, wherein no spectral features are observed when excited at 685 nm, unless both components are present in

solution. Similarly, the photographs in **Figure 4.4b** show that under 685 nm excitation luminescence is only observable in the rubrene/TSQ solution. This lack of emission is important because it demonstrates that the rubrene luminescence that we observe in the upconversion system is in no way due to two-photon absorption on rubrene at the illumination intensities used in this study.

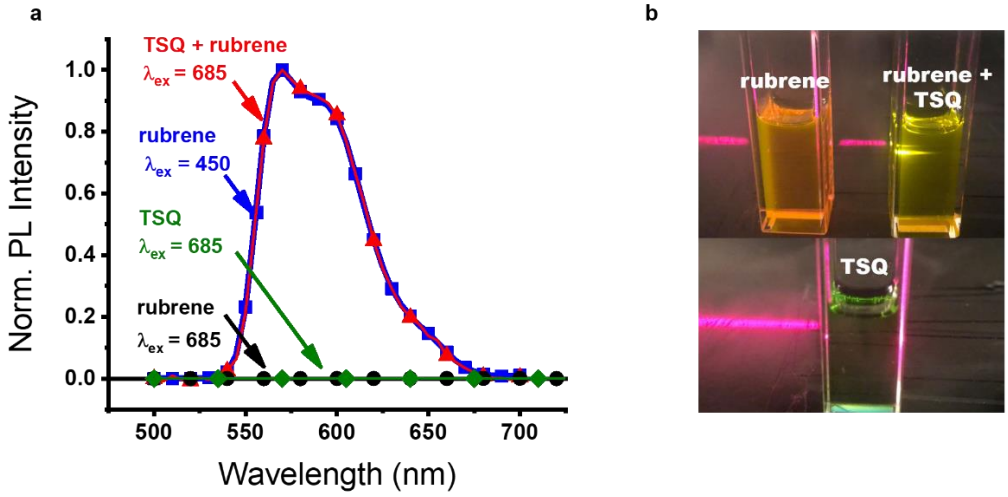

Figure 4.4. (a) In the upconversion sample, selective excitation of the thiosquaraine at 685 nm leads to upconverted fluorescence from the rubrene component. This fluorescence is identical to the fluorescence observed when rubrene is excited at 450 nm. No fluorescence is observed from either individual molecule when excited in isolation at λ_{ex} = 685 nm. (b) Photograph of upconverted emission resulting from 685 nm excitation, compared to individual components which show no emission with λ_{ex} = 685 nm excitation.

While **Figure 4.4** clearly demonstrates that the upconverted emission and the native rubrene emission are spectrally indistinguishable, the temporal responses of these two signals are markedly different. To study their disparate kinetics, we monitored the decay time for the upconverted rubrene emission and compared it to that of the native rubrene emission. The lifetime of the upconverted emission is significantly longer than the native rubrene fluorescence lifetime. In the upconversion sample, we observe an increase in the rubrene-centered luminescence decay time constant to a value of τ = 60 μs, in contrast to a value of τ = 0.016 μs

for the isolated rubrene fluorescence decay in solution (**Figure 4.5**). These results indicate that the decay time for the rubrene-centered emission in the upconversion sample is not governed by the radiative lifetime of the S_1/S_0 transition. Rather, the upconversion decay time depends on the rubrene triplet excited state decay time for the upconversion system.

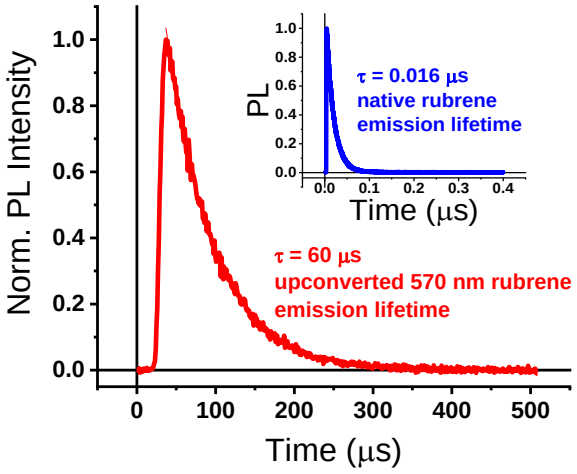

Figure 4.5. Lifetime data of the upconverted rubrene fluorescence, indicating a lifetime value of τ = 60 μs. The inset shows that the native rubrene fluorescence decays with a lifetime value of τ = 16 ns when excited at 470 nm in isolation.

In order to more carefully assess the excited state dynamics of our thiosquaraine upconversion system, we turned to a kinetic analysis based on ns to μs broadband-probe transient absorption spectroscopy. Transient absorption (TA) is a pump-probe spectroscopy which can monitor similar excited state absorption features to those revealed in our PIA spectroscopy but with the added advantage of reporting on kinetic evolution of the system directly in the time-domain. We note that similar dynamic information can be qualitatively gleaned from modulation frequency-dependent PIA spectroscopy measurements (**Figure A-2**). Nevertheless, broadband TA often affords one the added advantage of kinetically resolving characteristic spectral fingerprints that would otherwise be intractable to spectrally disentangle. Transient absorption measurements of

the neat thiosquaraine shown in **Figure 4.6a** exhibit a nearly identical induced absorption feature to that which we observed in cw-PIA studies at probe wavelengths near 590 nm. This induced absorption decays with a time constant of 20 μs (**Figure 4.6c**). Adding just 0.05 mM rubrene significantly decreases the time constant of this feature to 1.4 μs (**Figure 4.6c**), indicating a marked dynamic quenching of the TSQ triplet state. Additionally, the presence of rubrene leads to a new induced absorption feature from 480 – 510 nm, consistent with the rubrene triplet excited state,[30] shown in **Figure 4.6b**. This feature does not fully decay on the 35 μs timescale of the experiment (**Figure 4.6d**). The inset of **Figure 4.6b** shows a clear isosbestic point between the tail of the feature at 590 nm and the new feature at 495 nm. An isosbestic point is characteristic of interconversion between two species and provides strong evidence that triplet-triplet energy transfer occurs from the TSQ triplet state (^{3}TSQ) to rubrene triplet state (^{3}Rubrene).

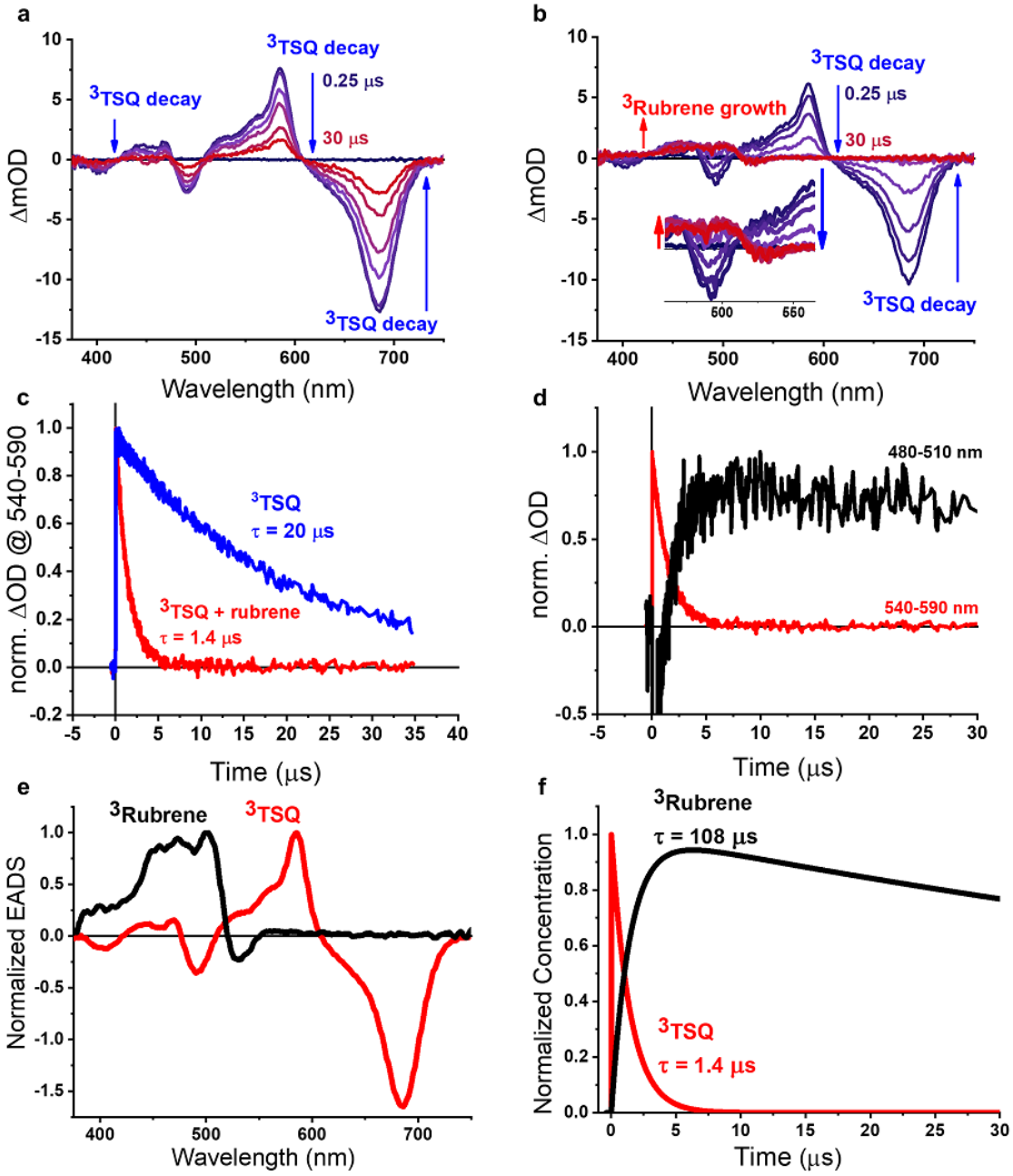

Figure 4.6. (a) Transient absorption spectrum of thiosquaraine in toluene, showing induced absorption feature at 590 nm associated with the triplet (b) Transient absorption spectrum of thiosquaraine in the presence of rubrene. A new induced absorption is observed from 480-510 nm associated with the rubrene triplet. (c) Kinetics of the thiosquaraine triplet absorption with and without the presence of rubrene, indicating dynamic quenching of the thiosquaraine triplet by rubrene. (d) Kinetics of the thiosquaraine triplet in the presence of rubrene compared to the kinetics of the rubrene triplet absorption. (e) Normalized species associated decay spectra of the thiosquaraine triplet and the rubrene triplet from global analysis (f) Kinetics of the rubrene and thiosquaraine triplet from global analysis.

While the isosbestic point that we observe in our ns to μs TA spectra for the thiosquaraine upconversion samples reports qualitatively on the triplet energy transfer process, as described above in the Methods section of this work, global analysis can provide quantitative information on the kinetics for this process. Global analysis fitting of the thiosquaraine/rubrene TA spectral evolution reveals the two spectral features shown in **Figure 4.6e**, the first belonging to the thiosquaraine triplet and the second belonging to the rubrene triplet. The EADS corresponding to the thiosquaraine triplet is identical to the spectrum observed in the absence of rubrene, shown in **Figure A-1**. The kinetic fits from Global analysis show the crossover time between the decay of the thiosquaraine triplet state and the rise of the rubrene triplet absorption (**Figure 4.6f**). This allows us to extract a time constant for the decay of the TSQ triplet and the rise of the rubrene triplet associated with the energy transfer process of τ = 1.4 μs. Through global analysis, the species associated with the rubrene triplet excited state is shown to decay with a 108 μs lifetime.

Having established the dynamic nature of the quenching process and the ^{3}TSQ lifetime in the absence of an external quencher, we set out to measure the concentration-dependence of the quenching to determine the quenching rate coefficient (k_Q) for the triplet energy transfer process. Stern-Volmer analysis is frequently used to quantitatively measure the quenching of the sensitizer triplet state by an annihilator molecule. For upconversion systems, especially those relying on metal complexes as sensitizers, phosphorescence quenching is most frequently used for Stern-Volmer analysis. Unfortunately, the we observed no measurable phosphorescence from the thiosquaraine molecule, which makes it intractable for us to perform a traditional Stern-Volmer quenching analysis based on luminescence quenching to determine k_Q. Nevertheless, similarly to our TA measurements, adding rubrene quenches the ^{3}TSQ induced absorption in our quasi-steady state photoinduced absorption measurement as well, shown in **Figure 4.7a**. This

effect allows us to utilize intensity quenching of this ^{3}TSQ induced absorption signature for a modified Stern-Volmer analysis (**Figure 4.7b**), as outlined in Equations 1 and 2:

$$\left(\frac{\Delta T}{T}\right)_0 / \left(\frac{\Delta T}{T}\right) = 1 + K_{SV}[Q] \quad \text{Eq. 1}$$

$$K_{SV} = k_Q * \tau_{^3TSQ} \quad \text{Eq. 2}$$

Here, $(\Delta T/T)_0$ is the native ^{3}TSQ absorption intensity in the absence of rubrene, $(\Delta T/T)$ is the ^{3}TSQ absorption intensity at each rubrene concentration, K_{SV} is the Stern-Volmer quenching constant, and [Q] is the concentration of the quencher. K_{SV} is a product of k_Q, the quenching constant, and $\tau_{^3TSQ}$, the triplet lifetime, taken from transient absorption (τ = 20 μs, **Figure 4.6c**). Thus, using the ratio of intensities of the photoinduced absorption triplet signal, with and without the presence of rubrene, and the native triplet lifetime we recover a value for the ^{3}TSQ quenching coefficient of $k_Q = 1.4 \times 10^9$ M^{-1} sec^{-1}. For this system, such a value for k_Q is roughly associated with diffusion-controlled quenching dynamics.

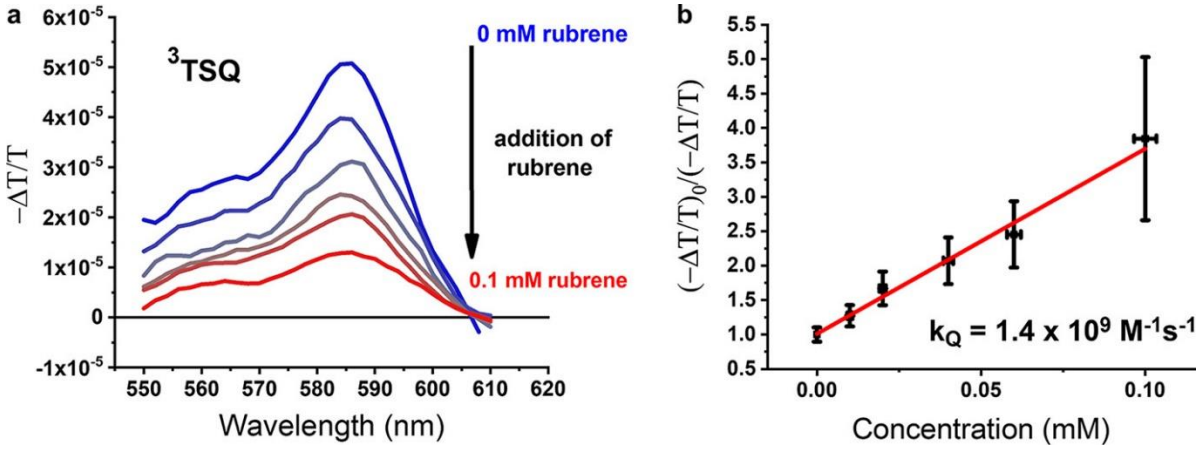

Figure 4.7. (a) Quasi-steady-state photoinduced absorption (PIA) spectra of thiosquaraine with rubrene concentrations ranging from 0.01 to 0.1 mM, revealing quenching of the thiosquaraine triplet. Spectra collected with photomodulation frequencies of 200 Hz. (b) Stern-Volmer analysis of the PIA quenching data in (a) returns a thiosquaraine triplet quenching rate constant of $k_Q = 1.4 \times 10^9$ M^{-1} s^{-1}

Since the cw-PIA measurements require the sample to be stable over an extended period of measurement time, typically anywhere between 30 minutes and 12 hours of illumination depending on the required signal-to-noise ratio, we also monitored the photostability of ^{3}TSQ absorption signal by tracking its intensity as a function of illumination time. As shown in **Figure A-3a**, the ^{3}TSQ absorption signal exhibits robust photostability, with no loss in upconversion intensity over a period of at least 10 hours of illumination. A similar experiment was run for the upconverted emission, showing photostability over a period of time in excess of 35 hours of illumination (**Figure A-3b**).

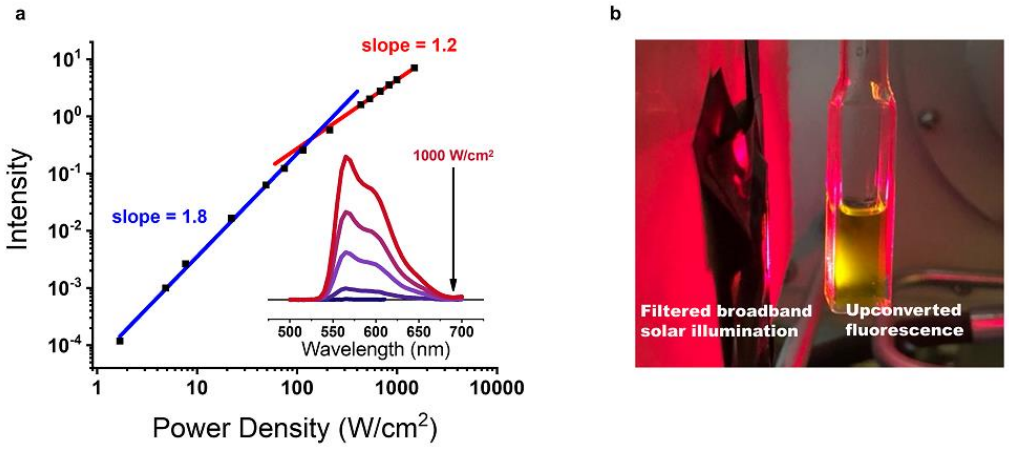

Figure 4.8. (a) Power dependence of the upconverted fluorescence detected at 585 nm under variable intensity 685 nm illumination. The sample exhibits a crossover point from nearly-quadratic to nearly-linear power dependence at roughly 150 W/cm^2. (b) Photographic image of upconverted fluorescence generated from filtered (650 nm longpass) simulated solar illumination.

As the TTA photon upconversion process outputs one high-energy photon from two input low-energy photons, the upconverted emission intensity will have a quadratic dependence on the ncident power density in the weak annihilation limit. However, as the pseudo-first order rate constant of the triplet acceptor decay becomes much larger than the rate constant of the second order TTA process, the emission intensity will exhibit a linear relationship to incident power

density.[31] This saturation limit is important for determining the most efficient power density for the upconversion process, as well as for evaluating the practicality of a system for solar applications, where the incident power density is low.

The power dependence of the upconverted rubrene fluorescence shown in **Figure 4.8a** was measured in the presence of thiosquaraine as a function of 685 nm incident optical power density. The luminescence intensity of the upconversion sample exhibits a quadratic power dependence below roughly 150 W/cm^2 optical power density, where a crossover point into the strong annihilation limit is evident in the double-logarithmic plot in **Figure 4.8a**. While the strong annihilation region represents the range of input laser fluences wherein the upconversion process is the most efficient, we note that we do in fact observe upconverted fluorescence when the sample is excited by a solar simulator with a 650 nm longpass filter on the output, as shown in **Figure 4.8b**.

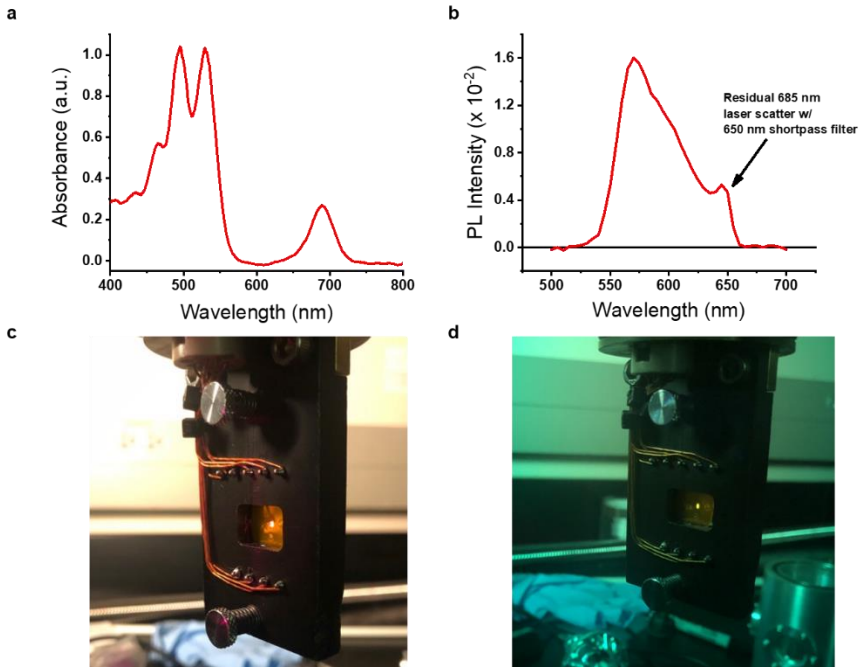

Figure 4.9. (a) Absorbance spectrum of a representative thiosquaraine/rubrene film in an ethylene oxide-epichlorohydrin (EO-EPI) copolymer. (b) Emission spectrum of the thiosquaraine rubrene EO-EPI film. (c) Photograph of the thiosquaraine/rubrene EO-EPI film under 685 nm excitation, taken in aerobic conditions. (d) Photograph of the upconverted emission under 685 nm excitation taken through a 600 nm shortpass filter.

For facile integration into a solid-state photovoltaic device, it is generally ideal that the upconversion system be active in a thin-film architecture. TTA upconversion relies on Dexter energy transfer, which fundamentally operates via an electron exchange mechanism. Therefore, TTA upconversion requires some degree of direct orbital overlap among the relevant chromophores. In practical terms, this means that a thin-film composite that supports TTA upconversion must accommodate molecular mobility so that the collisional events necessary for the electron exchange process can occur. Therefore, most strategies for transferring an upconversion system to the solid-state involve dispersion within an elastic polymer matrix. Several such materials, including polyurethanes,[25-26, 32] polyacrylates,[33] and ethylene oxide-epichlorohydrin (EO-EPI) copolymers,[27-28] have been investigated previously as hosts for solid-

state upconversion systems. Here, we selected an EO-EPI copolymer as a host matrix for the thiosquaraine/rubrene system based on chemical compatibility and film processing considerations. A representative absorption spectrum of the resulting upconversion film is displayed in **Figure 4.9a**. Solid-state photon upconversion is readily apparent from the thin-film sample following illumination of the thiosquaraine component with 685 nm laser diode. The spectrum of the thin-film upconversion emission is reported in **Figure 4.9b**. We note that this spectrum was measured with a 650 nm shortpass filter following the sample and before the detector. Due to the slightly scattering nature of the thin-film sample and the nominal 10 nm FWHM bandwidth of the excitation beam, a slight shoulder appears on the red edge of the thin-film upconversion profile, which is due to scattering of the laser diode tail. The solid-state luminescence from this thin-film upconversion platform is intense enough to be readily observed by eye, even in an aerobic environment, conditions in which one might initially anticipate oxygen quenching. Nevertheless, the photographic images in **Figure 4.9c** (no optical filtering) and **Figure 4.9d** (image taken through a 600 nm shortpass filter) clearly demonstrate strong red-to-yellow photon upconversion in air for these completely heavy atom-free thin-films.

4.3 CONCLUSIONS

Stringent scalability and economic challenges persist in the face of emerging and established solar photovoltaic systems. New, potentially cost-effective, photon upconversion platforms, aimed at routinely meeting, or possibly exceeding, the Shockley-Queisser efficiency limit for the solar energy conversion efficiency of these systems are becoming increasingly compelling. As one recent example, herein we have presented a successful triplet-triplet annihilation photon upconversion platform that utilizes a molecular, heavy atom-free, thionated squaraine dye sensitizer that is capable of promoting intense thin-film upconversion luminescence,

even under aerobic conditions. Given the broad electronic diversity that is accessible through chemical functionalization of the squaraine platform, we anticipate that devices based on this initial thin-film demonstration will gain viability as a model testbed for developing metal-free organic sensitizers for solar upconversion applications. In particular, the highly-tunable squaraine motif can be modified to push the absorption well into the NIR. For solar applications, the ideal triplet sensitizers would absorb in the deep red to NIR, as this region of the solar spectrum is poorly utilized by traditional semiconductor materials used in photovoltaics[34] and emerging thin-film materials such as organometal halide perovskites. In comparison to our system, some success has also been achieved using thionation to increase the intersystem crossing efficiency of perylene diimides (PDI).[35] The PDI absorption can be shifted into the NIR by extending the size of the fused ring system.[36] However, this massive π-extension can lead to substantial aggregation and severe materials processing challenges. While adding sterically-blocking bulky substituents is an effective strategy for circumventing this problem, such modifications are unattractive for TTA upconversion due to the orbital overlap and molecular collisions that are required for the Dexter energy transfer process to occur, particularly in a thin-film architecture. On the other hand, the squaraine absorption features are predominately achieved by the push-pull nature of its intramolecular charge-transfer type transitions.[37] As such, achieving NIR absorption with a functionalized squaraine sensitizer need not negatively impact its processing. Correspondingly, thiosquaraines appear to present an exciting new parameter space for implementing NIR photon upconversion in multiple potential applications, from photodetectors and solar cells to imaging and sensing.

4.4 REFERENCES

1. Shockley, W.; Queisser, H. J., *J. Appl. Phys.* **1961,** *32*, 510-519.

2. Frazer, L.; Gallaher, J. K.; Schmidt, T. W., *ACS Energy Lett.* **2017,** *2*, 1346-1354.

3. Schulze, T. F.; Czolk, J.; Cheng, Y.-Y.; Fückel, B.; MacQueen, R. W.; Khoury, T.; Crossley, M. J.; Stannowski, B.; Lips, K.; Lemmer, U.; Colsmann, A.; Schmidt, T. W., *J. Phys. Chem. C.* **2012,** *116*, 22794-22801.

4. Cheng, Y. Y.; Nattestad, A.; Schulze, T. F.; Macqueen, R. W.; Fückel, B.; Lips, K.; Wallace, G. G.; Khoury, T.; Crossley, M. J.; Schmidt, T. W., *Chem. Sci*. **2015,** *7*, 559-568.

5. Ha, S. J.; Kang, J. H.; Choi, D. H.; Nam, S. K.; Reichmanis, E.; Moon, J. H., *ACS Photonics* **2018,** *5*, 3621-3627.

6. Khnayzer, R. S.; Blumhoff, J.; Harrington, J. A.; Haefele, A.; Deng, F.; Castellano, F. N., *Chem. Comm.* **2012,** *48*, 209-211.

7. Islangulov, R. R.; Castellano, F. N., *Angew. Chem. Int. Ed.* **2006,** *45*, 5957-5959.

8. Zhou, N.; Xu, B.; Gan, L.; Zhang, J. P.; Han, J. B.; Zhai, T. Y., *J. Mater. Chem. C.* **2017,** *5* (7), 1591-1595.

9. Liu, Q.; Xu, M.; Yang, T.; Tian, B.; Zhang, X.; Li, F., *ACS Appl. Mater. Interfaces* **2018,** *10*, 9883-9888.

10. Singh-Rachford, T. N.; Castellano, F. N., *Coord. Chem. Rev.* **2010,** *254*, 2560-2573.

11. Cui, X.; Zhao, J.; Yang, P.; Sun, J., *Chem. Comm.* **2013,** *49*, 10221-10223.

12. Castellano, F. N.; Singh-Rachford, T. N., *J. Phys. Chem. A.* **2008,** *112* (16), 3550-3556.

13. Kimizuka, P. D.; Nobuhiro, Y.; Nobuo, *Chem. Comm.* **2014,** *50*, 13111-13113.

14. Ji, S.; Guo, H.; Wu, W.; Wu, W.; Zhao, J., *Angew. Chem. Int. Ed.* **2011,** *50*, 8283-8286.

15. Gouterman, M., *J. Mol. Spectrosc.* **1961,** *6*, 138-163.

16. Rogers, J. E.; Cooper, T. M.; Fleitz, P. A.; Glass, D. J.; McLean, D. G., *J. Phys. Chem. A.* **2002,** *106*, 10108-10115.

17. Wu, W.; Guo, H.; Wu, W.; Ji, S.; Zhao, J., *J. Org. Chem.* **2011,** *76*, 7056-7064.

18. Yanai, N.; Kimizuka, N., *Acc. Chem. Res.* **2017,** *50*, 2487-2495.

19. Yang, D. W.; Fan, N.; Zece, Z.; Yang, Z.; Chuluo, *J. Mater. Chem. C.* **2017,** *5*, 12674-12677.

20. Castellano, T. N. S.-R.; Felix, N., *J. Phys. Chem. A.* **2009,** *113* (20), 5912-5917.

21. Zhao, J.; Chen, K.; Hou, Y.; Che, Y.; Liu, L.; Jia, D., *Org. Biomol. Chem.* **2018,** *16*, 3692-3701.

22. Manna, M. K.; Shokri, S.; Wiederrecht, G. P.; Gosztola, D. J.; Ayitou, A. J.-L., *Chem. Comm.* **2018,** *54*, 5809-5818.

23. Peceli, D.; Hu, H.; Fishman, D. A.; Webster, S.; Przhonska, O. V.; Kurdyukov, V. V.; Slominsky, Y. L.; Tolmachev, A. I.; Kachkovski, A. D.; Gerasov, A. O.; Masunov, A. E.; Hagan, D. J.; Van Stryland, E. W., *J. Phys. Chem. A.* **2013,** *117*, 2333-2346.

24. Webster, S.; Peceli, D.; Hu, H.; Padilha, L. A.; Przhonska, O. V.; Masunov, A. E.; Gerasov, A. O.; Kachkovski, A. D.; Slominsky, Y. L.; Tolmachev, A. I.; Kurdyukov, V. V.; Viniychuk, O. O.; Barrasso, E.; Lepkowicz, R.; Hagan, D. J.; Van Stryland, E. W., *J. Phys. Chem. Lett.* **2010,** *1*, 2354-2360.

25. Kim, J. H.; Deng, F.; Castellano, F. N.; Kim, J. H., *Chem. Mater*. **2012,** *24*, 2250-2252.

26. Hagstrom, A. L.; Lee, H.-L.; Lee, M.-S.; Choe, H.-S.; Jung, J.; Park, B.-G.; Han, W.-S.; Ko, J.-S.; Kim, J.-H.; Kim, J.-H., *ACS Appl. Mater. Interfaces* **2018,** *10*, 8985-8992.

27. Islangulov, R. R.; Lott, J.; Weder, C.; Castellano, F. N., *J. Am. Chem. Soc.* **2007,** *129*, 12652-12653.

28. Singh-Rachford, T. N.; Lott, J.; Weder, C.; Castellano, F. N., *J. Am. Chem. Soc.* **2009,** *131*, 12007-12014.

29. El-Sayed, M. A., *J. Chem. Phys.* **1963,** *38*, 2834-2838.

30. Porter, G.; Windsor, M. W., *Proc. R. Soc. Lond. A.* **1958,** *245*, 238-258.

31. McCusker, C. E.; Castellano, F. N., *Chem. Comm.* **2013,** *49*, 3537-3539.

32. Li, C.; Koenigsmann, C.; Deng, F.; Hagstrom, A.; Schmuttenmaer, C. A.; Kim, J. H., *ACS Photonics* **2016,** *3*, 784-790.

33. Monguzzi, A.; Mauri, M.; Bianchi, A.; Dibbanti, M. K.; Simonutti, R.; Meinardi, F., *J. Phys. Chem. C.* **2016,** *120*, 2609-2614.

34. Gray, V.; Dzebo, D.; Abrahamsson, M.; Albinsson, B.; Moth-Poulsen, K., *Phys. Chem. Chem. Phys.* **2014,** *16*, 10345-10352.

35. Tilley, A. J.; Pensack, R. D.; Lee, T. S.; Djukic, B.; Scholes, G. D.; Seferos, D. S., *J. Phys. Chem. C.* **2014,** *118*, 9996-10004.

36. Avlasevich, Y.; Li, C.; Müllen, K., *J. Mater. Chem.* **2010,** *20*, 3814-3826.

37. Law, K. Y., *J. Phys. Chem.* **1987,** *91*, 5184-5193.

Chapter 5. Record Red-to-Blue Triplet-Triplet Annihilation Upconversion with a Heavy-Atom-Free Thiosquaraine Sensitizer

5.1 Introduction

Photon upconversion has attracted recent research interest due to its potential for use in photonic applications, including photovoltaics,[1-4] photocatalysis,[5-6] bioimaging,[7] and sensing.[8] Triplet-triplet annihilation (TTA) or triplet fusion upconversion is a particularly attractive mechanism of upconversion due to the large tunability of spectral ranges, low incident power density requirements, and the potential for broadband excitation. TTA upconversion involves a sensitizer and emitter molecule in solution or a solid-state matrix. The sensitizer molecule is excited, undergoes intersystem crossing to the triplet state, and subsequently experiences triplet-triplet energy transfer (TTET) to the emitter molecule. Two emitter triplets can then annihilate, deactivating one to the ground state and promoting one to an excited singlet state in an overall spin-allowed process. This excited singlet then fluoresces at an energy higher than the incident photon excitation. **Figure 5.1** summarizes this mechanism.

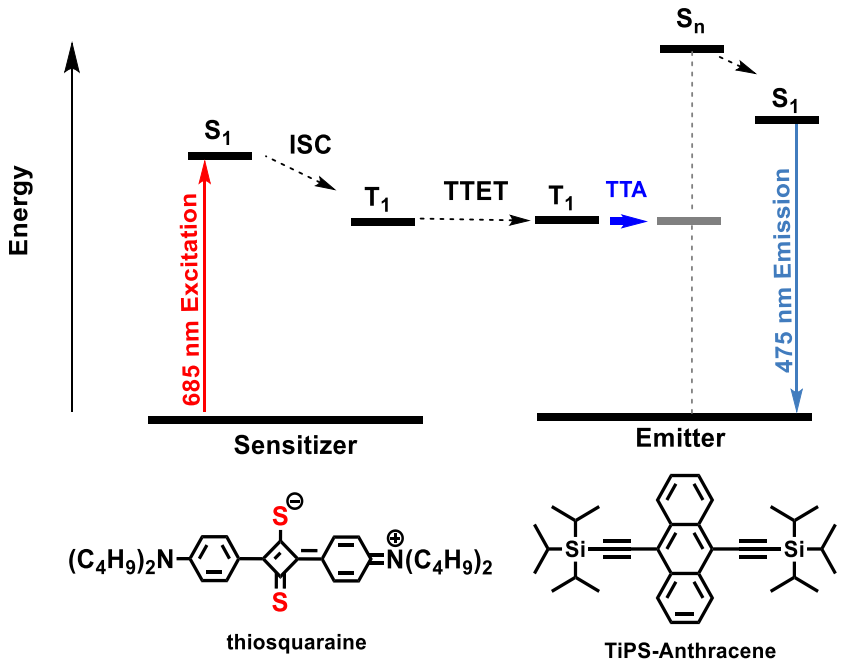

Figure 5.1. Triplet–triplet annihilation (TTA) upconversion mechanism. The excitation wavelength of our thiosquaraine (TSQ) system presented herein is 685 nm. The peak of the upconverted TiPS-Anthracene-centered emission is at 475 nm. The chemical structures of the TSQ sensitizer and the TiPS-Anthracene emitter are shown.

One important factor that determines whether a TTA upconversion system is suitable for a given application is the apparent anti-Stokes shift, or the energy difference between the excitation and upconverted emission energies (ΔE_{UC}). For photovoltaic applications, photons need only to be upconverted to energies slightly greater than the band gap energy of the active material. Any additional energy will be lost as heat through thermalization to the band edge energy.[9] On the other hand, higher-energy blue or ultraviolet photons are typically required to drive the photochemical reactions used to generate solar fuels.[5, 10-11] In this respect, larger energy shifts are attractive, with TTA upconversion providing the opportunity to drive these reactions with lower energy photons that are prevalent in incident solar flux. However, large ΔE_{UC} values are traditionally difficult to achieve, chiefly due to the energy losses at each step of the TTA-UC process (Scheme 1).

Most traditional TTA photon upconversion systems have relied on precious heavy metal complexes[12-15] or photolabile halogen atoms[16] to induce the necessary spin orbit coupling in the sensitizer molecules. Incorporating these costly precious metals may ultimately constitute an additional barrier to widespread adoption. Previously, we have reported an all-organic, heavy-atom-free, TTA upconversion system utilizing a thionated squaraine dye as the sensitizer.[17] Substituting sulfur for oxygen on the squaraine core reorders the lowest energy singlet states, opening a channel for intersystem crossing, as expected based on El-Sayed's Rule.[18-19] Here we report an increased apparent anti-Stokes shift for our thiosquaraine upconversion system by demonstrating red-to-blue upconversion from the thiosquaraine paired with a TiPS-Anthracene emitter. This system has a peak-to-peak ΔE_{UC} of 0.80 eV, which, to our knowledge, is the largest anti-Stokes shift reported in any heavy-atom-free system and the second largest anti-Stokes shift in a metal-free system.[20]

5.2 Results and Discussion

Our thiosquaraine (TSQ) sensitizer exhibits an intense absorption band (1.57×10^5 M^{-1} cm^{-1}) in the deep red at 685 nm (**Figure 5.2**). Our previous work demonstrated efficient triplet energy transfer from the thiosquaraine sensitizer to rubrene, which emits in the yellow region of the spectrum (λ_{max} = 570 nm). After considering an array of potential emitter molecules to extend the apparent anti-Stokes shift of the upconverted emission into the blue region, we selected 9,10-bis[(triisopropylsilyl)ethynyl]anthracene (TiPS-An, **Figure 5.2**). TiPS-An has an emission maximum at 450 nm in dilute solution (**Figure 5.2**), making it an attractive candidate to achieve red-to-blue upconversion with our thiosquaraine sensitizer. The TiPS-An absorption profile is also spectrally distinct from the thiosquaraine absorption band, allowing us to selectively excite the sensitizer component. A previous study by Pun et al. demonstrated TTA upconversion using

platinum octaethylporphyrin (PtOEP, $\varepsilon_{ex} = 3.55 \times 10^4\ M^{-1}\ cm^{-1}$, $\lambda_{max} = 530$ nm) as a sensitizer for TiPS-An.[21] More recently, a study by Nishimura et al. showed efficient upconversion to TiPS-An from Pd(II) meso-tetraphenyltetrabenzoporphine (PdTPBP, $\varepsilon_{max} = 1.1 \times 10^5\ M^{-1}\ cm^{-1}$, $\lambda_{max} = 628$ nm). Also in this study, the authors sensitize TiPS-An with direct excitation of a very low oscillator strength S_0 to T_1 transition in PtTPBP ($\lambda_{ex} = 785$ nm, $\lambda_{max} = 614$ nm). [22]

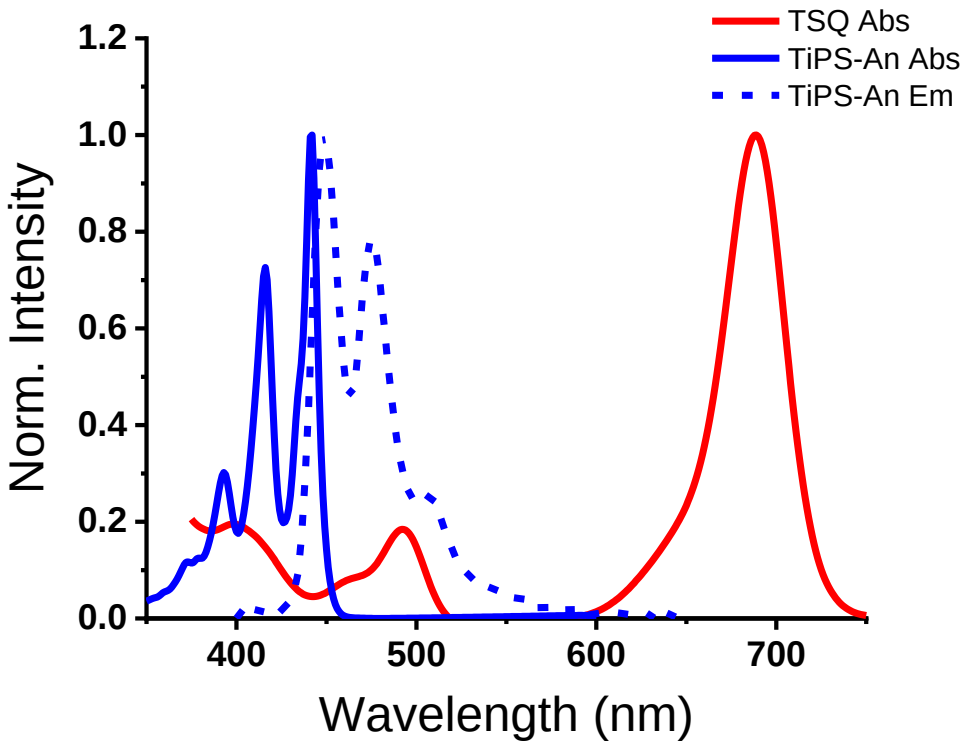

Figure 5.2 Absorption (solid blue line) and emission (dashed blue line) characteristics of TiPS-Anthracene compared with the thiosquaraine absorption spectrum (solid red line).

Figure 5.3a shows that selectively exciting the thiosquaraine molecule with 685 nm red light in solution with TiPS-An results in upconverted blue fluorescence. The upconverted emission that we observe is spectrally indistinguishable from the native singlet emission of TiPS-An at the same concentration following 365 nm excitation. **Figure 5.3a** also shows that we observe no emission with 685 nm excitation unless both components are present in solution. This

lack of emission is important because it demonstrates that the upconverted TiPS-An luminescence is in no way due to two-photon absorption on TiPS-An at the illumination intensities used in this study. The photograph in **Figure 5.3b** shows the blue upconverted emission resulting from the red excitation when both components are present in solution.

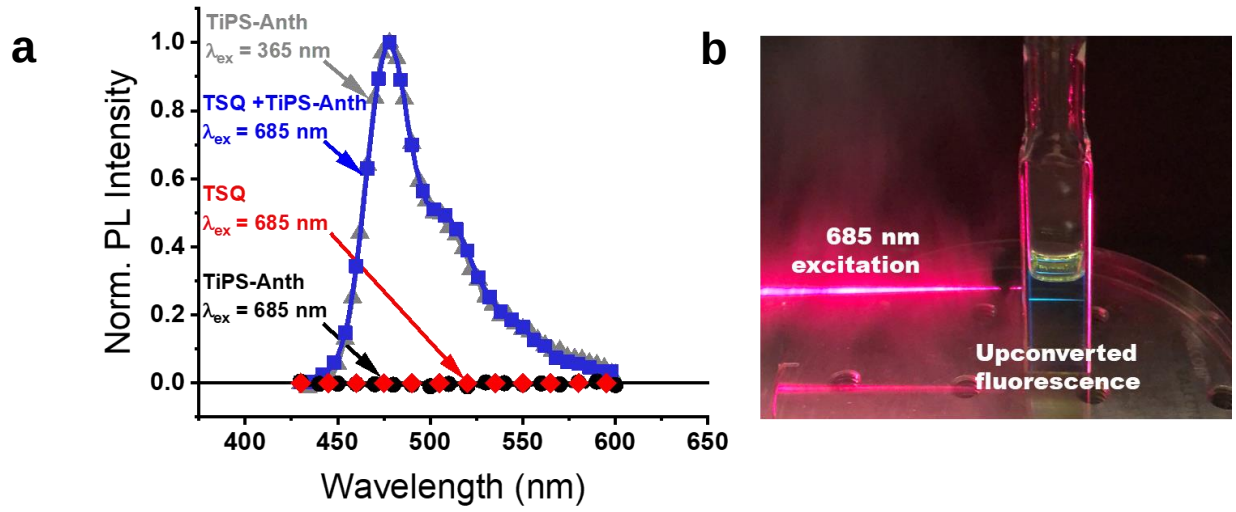

Figure 5.3. (a) In a TSQ/TiPS-An sample, selective excitation of the TSQ at 685 nm leads to upconverted fluorescence from the TiPS-An component. This fluorescence is identical to the fluorescence observed when TiPS-An is excited at 365 nm. No fluorescence is observed from either individual molecule when excited in isolation at λex = 685 nm. (b) Photograph of upconverted emission resulting from 685 nm excitation.

Significant variations still exist in the formalisms employed for calculating numerical values for anti-Stokes shifts (ΔE_{UC}) of TTA upconversion system in the literature. A commonly adopted method is to measure the energy shift from the excitation wavelength to upconverted emission wavelength. Since the excitation will be strongest at the peak absorption, we adopt the formalism to report the peak-to-peak upconversion margin, as done in the previous study by Cheng et. al.[23] This formalism has the added advantage of being based on the properties of the molecule and is thus standard across any given samples of the same formulation, unlike excitation wavelength which can vary based on instrumentation. Based on this approach, the

ΔE_{UC} of our red-to-blue upconversion system is 0.80 eV, which, to our knowledge, is higher than that reported for any heavy-atom-free system.[16, 24-25] This represents a 0.43 eV increase in peak-to-peak upconversion margin over our previous system.

It is important to note that we previously reported the anti-Stokes shift of our TSQ/rubrene system based on intensity-weighted averages of the upconverted emission and sensitizer absorption spectra, denoted as the upconversion energy shift (UES) by Gray et al.[26] Through this formalism, the UES of the TSQ/TiPS-An system is 0.65 eV, an increase of 0.38 eV over our previous system.[17] We include this additional method of reporting the energy shift in an effort to provide a more standardized comparison of these measurements across the field of TTA upconversion.

It is also noteworthy to mention that the upconversion can be driven on the red edge of the absorption profile of the thiosquaraine. This is particularly relevant as deep red or NIR excitations are desired for a number of upconversion applications, including photovoltaics and bioimaging, while most current upconversion systems are limited to visible-to-visible upconversion.[6] We have demonstrated upconversion luminescence from TiPS-An using 730 nm excitation of the thiosquaraine sensitizer, shown in **Figure B-1.** Upconverted fluorescence from TiPS-Anthracene by 730 nm excitation of the thiosquaraine sensitizer. This is one of the few reported examples of >700 nm excitation resulting in <500 nm emission in any upconversion system.[1-2]. The extinction coefficient at this wavelength is 1.57×10^4 M^{-1} cm^{-1}, a tenth of the maximum extinction coefficient, but notably is still on the order of magnitude of the extinction coefficient of a more traditional sensitizer like PtOEP. Using the red edge of the thiosquaraine absorption, this system becomes one of very few TTA upconversion examples of > 700 nm excitation resulting in < 500 nm emission.[6, 27]

As is typical of TTA upconversion systems, the upconverted fluorescence exhibits significantly different kinetics than that of the native emitter fluorescence. In the upconversion sample, we observe a decay constant of 71 μs for the TiPS-An centered fluorescence (**Figure 5.4**). This is in contrast to the reported decay constant of 6.6 ns for the native TiPS-An fluorescence.[21] Details of the upconversion lifetime measurement can be found in the Supporting Information.

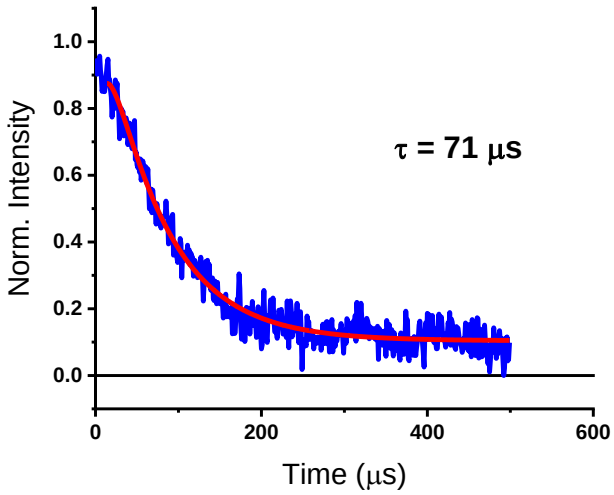

Figure 5.4. Kinetic trace of the upconverted emission of the TSQ/TiPS-An system (λ_{ex} = 685 nm). The upconverted emission lifetime of 71 μs is significantly extended from the native TiPS-An lifetime of 6.6 ns.

Both time-resolved transient absorption (TA) and quasi-steady state photoinduced absorption (PIA) measurements were undertaken to study the extent of quenching of the TSQ triplet by the addition of TiPS-An. Both measurements show that the quenching efficiency in the red-to-blue TSQ/TiPS-An system is diminished compared to the TSQ/rubrene system, where the quenching constant is on the order of the diffusion limit in toluene (k_Q = 1.4 x 10^9 M^{-1} s^{-1}).[17] With the TSQ/TiPS-An system, the quasi-steady state measurement intensity of the ^{3}TSQ feature is only marginally diminished, even when large concentrations (~20 mM) of acceptor are used (**Figure 5.5a**). We only observe significant quenching near the TiPS-An solubility limit, where

photoluminescence data indicates that aggregation has caused a bathochromic shift in the excited state energy. At this concentration, the luminescence maximum shifts from 475 nm to 550 nm and the luminescence spectrum is broadened, as shown in **Figure 5.5b**. Similar to the PIA measurements, the TA data also indicates a diminished quenching efficiency when compared to our previous system. Again, at large concentrations of acceptor, only a small amount of quenching is seen in the ^{3}TSQ lifetime, with the lifetime decreasing only to 15 μs from the 20 μs native triplet lifetime (**Figure 5.5d**).

The reduced TTET efficiency in the TSQ/TiPS-An system is likely due to the high triplet energy of TiPS-An inhibiting the triplet-triplet energy transfer process. The triplet of TiPS-An is reported to be ≥ 1.41 eV,[21] which is significantly higher than that of the rubrene triplet (E_T = 1.12 eV),[17] with which we previously demonstrated upconversion. In fact, the reported TiPS-An triplet energy is about 120 meV **larger** than the calculated triplet energy of the thiosquaraine (E_T = 1.29 eV).[19] These nearly isoenergetic triplet states minimize the energy loss through TTET of the system, allowing for the large upconversion energy shift but evidently impart an efficiency-limiting influence on the upconversion process. Given the prospect that the TiPS-An triplet energy lies at or above that of the TSQ triplet energy, it is possible that the quenching is masked by reverse triplet-triplet energy transfer processes.

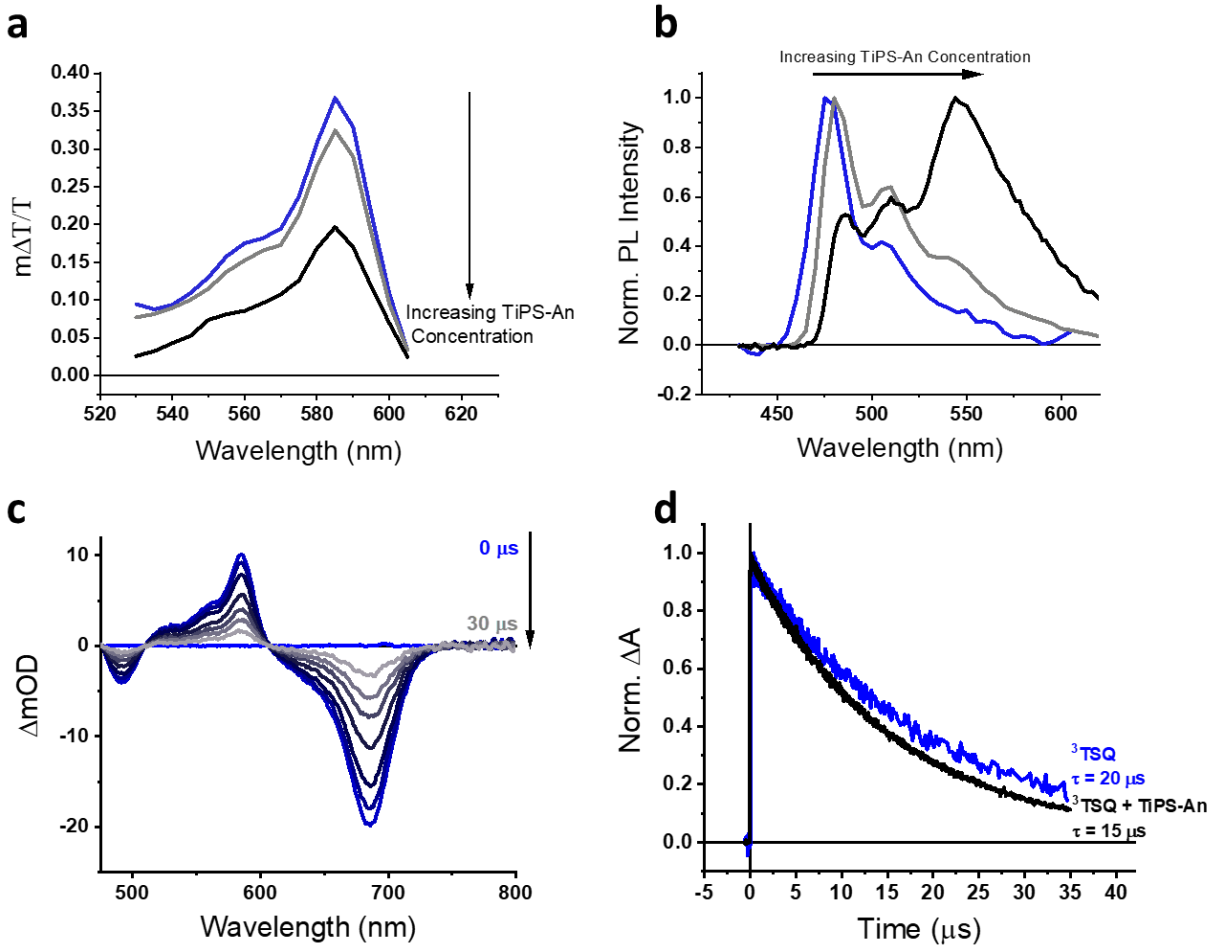

Figure 5.5. (a) Quasi-steady-state photoinduced absorption (PIA) spectra of the thiosquaraine triplet at varying TiPS-An concentrations. Large concentrations (gray trace) show minimal quenching of the ^{3}TSQ feature. More significant quenching is observed at the solubility limit (yellow trace), however, the photoluminescence data (b) indicates that at this concentration the acceptor has aggregated, and the energetic landscape has changed. (c) Transient absorption spectrum of the thiosquaraine in the presence of TiPS-An. (d) Kinetic traces of the triplet absorption with and without TiPS-An, showing minimal quenching.

To explore whether the triplet-triplet energy transfer process is indeed endothermic between TSQ and TiPS-An, the temperature dependence of the upconverted emission was measured. Over a range of 20° C to 50° C, the TiPS-An upconverted emission increased in intensity with increasing temperature, as shown in **Figure 5.6**. This is in contrast with the rubrene upconversion intensity, which decreased with increasing temperature over the same range (**Figure B-5**). Control measurements of the TiPS-An fluorescence do not show a

dependence on temperature in this range (**Figure B-4**). These data suggest that the triplet energy transfer process from TSQ to TiPS-An is thermally activated.

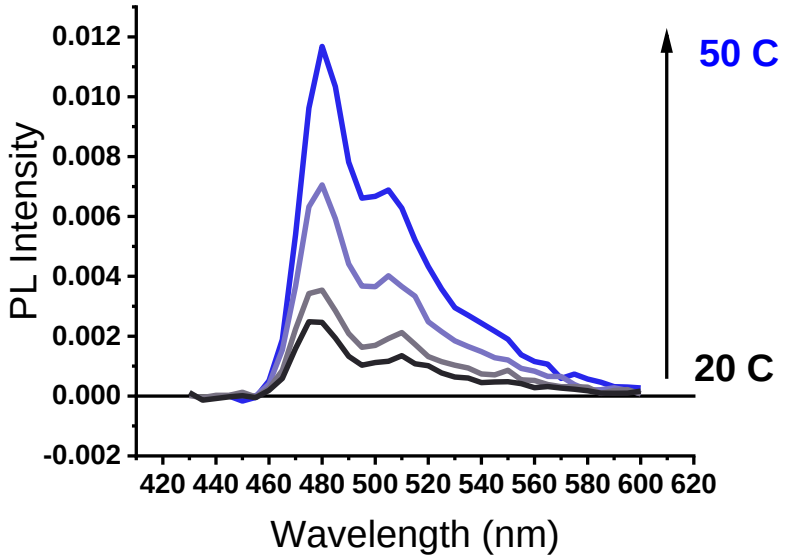

Figure 5.6. (a) Temperature dependent luminescence traces for the TSQ/TiPS-An upconversion system. As the temperature increases from 20˚C to 50˚C, the luminescence intensity increases by nearly an order of magnitude.

While the room-temperature upconversion efficiency of the TSQ/TiPS-An system is somewhat limited by the high E_T of the acceptor, this gives further insight into the energetic landscape of the thiosquaraine, as well as sets an upper bound for the energetic shifts possible with the current system. Since red-to-blue upconversion was achievable with the thiosquaraine sensitizer, we surmised that this same sensitizer could be easily paired with an alternate acceptor that would produce green emission upon red excitation. For this red-to-green upconversion we selected 1-chloro-bis(phenylethynyl) anthracene (1CBPEA) as the emitter. 1CBPEA has a reported triplet energy of 1.20 eV and has previously been used as an acceptor molecule in metal-free upconversion schemes using iodinated BODIPY sensitizers.[16] When pairing 1CBPEA with TSQ, green emission centered at 530 nm is detected under 685 nm excitation (**Figure 5.7**).

No emission is observed unless both components are present in solution (**Figure B-6**). This initial characterization further demonstrates the range of the thiosquaraine sensitizer. Understanding the energetic limitations of the TSQ upconversion system is also useful to inform annihilator selection as we move to design thiosquaraine derivatives that absorb further into the NIR. Maintaining useful visible or deep-red emission requires that the E_T of the emitter molecule not drop below ½ the desired singlet energy. However, as the sensitizer energy is lowered, this will result in decreased enthalpic driving forces for TTET. This study shows that an important consideration in selection of emitters for NIR-absorbing sensitizers will be the trade-off between efficient TTET and the emission energy.

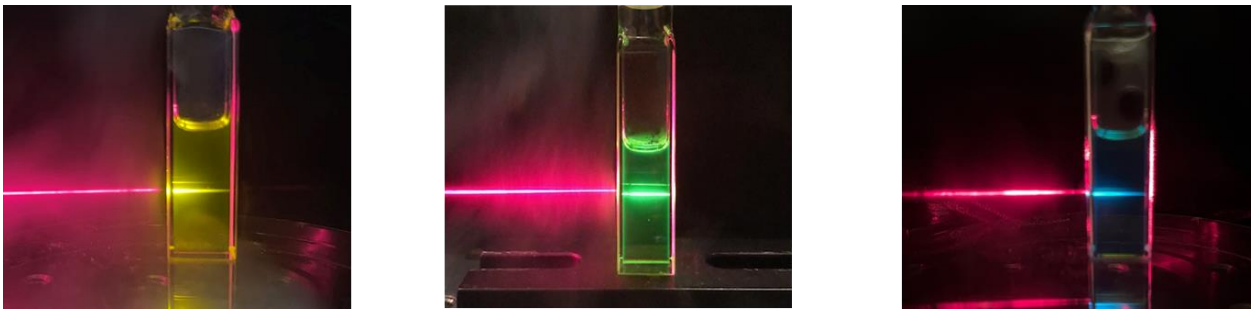

Figure 5.7. Photographic demonstration of (a) red-to-yellow upconversion using TSQ/rubrene system (b) red-to-green upconversion using TSQ/1CBPEA system, and (c) red-to-blue upconversion using TSQ/TiPS-An system.

5.3 CONCLUSIONS

Triplet-triplet annihilation upconversion has the potential to meaningfully impact a number of photonics applications, but heavy-atom-free sensitizers will be needed to make the systems economical for large scales. Herein, we have shown that our previously reported thiosquaraine sensitizer can be paired with TiPS-Anthracene in order to produce photon upconversion with the largest demonstrated anti-Stokes shift in heavy-atom-free systems. The

increase in anti-Stokes shift is driven by an increase in the emitter triplet energy, resulting in an energetically uphill triplet-triplet energy transfer from the thiosquaraine. The apparent thermally activated nature of the system is evident through an increase in quenching efficiency and upconversion emission efficiency with increasing sample temperature. Increasing the anti-Stokes shift of the system opens the application space to include various photochemical systems such as photocatalytic reactions of solar fuels or novel drug delivery systems.[20]

1. Frazer, L.; Gallaher, J. K.; Schmidt, T. W., *ACS Energy Lett.* **2017,** *2*, 1346-1354.

2. Schulze, T. F.; Czolk, J.; Cheng, Y.-Y.; Fückel, B.; MacQueen, R. W.; Khoury, T.; Crossley, M. J.; Stannowski, B.; Lips, K.; Lemmer, U.; Colsmann, A.; Schmidt, T. W., *J. Phys. Chem. C.* **2012,** *116*, 22794-22801.

3. Cheng, Y. Y.; Fückel, B.; MacQueen, R. W.; Khoury, T.; Clady, R. G. C. R.; Schulze, T. F.; Ekins-Daukes, N. J.; Crossley, M. J.; Stannowski, B.; Lips, K.; Schmidt, T. W., *Energy and Environmental Science* **2012,** *5*, 6953-6959.

4. Ha, S. J.; Kang, J. H.; Choi, D. H.; Nam, S. K.; Reichmanis, E.; Moon, J. H., *ACS Photonics* **2018,** *5*, 3621-3627.

5. Islangulov, R. R.; Castellano, F. N., *Angew. Chem. Int. Ed.* **2006,** *45*, 5957-5959.

6. Bharmoria, P.; Bildirir, H.; Moth-Poulsen, K., *Chem. Soc. Rev.* **2020,** *49*.

7. Liu, Q.; Xu, M.; Yang, T.; Tian, B.; Zhang, X.; Li, F., *ACS Appl. Mater. Interfaces* **2018,** *10*, 9883-9888.

8. Zhou, N.; Xu, B.; Gan, L.; Zhang, J. P.; Han, J. B.; Zhai, T. Y., *J. Mater. Chem. C.* **2017,** *5* (7), 1591-1595.

9. Shockley, W.; Queisser, H. J., *J. Appl. Phys.* **1961,** *32*, 510-519.

10. Corp, K. L.; Schlenker, C. W., *J. Am. Chem. Soc.* **2017,** *139*, 7904-7912.

11. Rabe, E. J.; Corp, K. L.; Sobolewski, A. L.; Domcke, W.; Schlenker, C. W., *J. Phys. Chem. Lett.* **2018,** *9*, 6257-6261.

12. Singh-Rachford, T. N.; Castellano, F. N., *Coord. Chem. Rev.* **2010,** *254*, 2560-2573.

13. Cui, X.; Zhao, J.; Yang, P.; Sun, J., *Chem. Comm.* **2013,** *49*, 10221-10223.

14. Castellano, F. N.; Singh-Rachford, T. N., *J. Phys. Chem. A.* **2008,** *112* (16), 3550-3556.

15. Kimizuka, P. D.; Nobuhiro, Y.; Nobuo, *Chem. Comm.* **2014,** *50*, 13111-13113.

16. Wu, W.; Guo, H.; Wu, W.; Ji, S.; Zhao, J., *J. Org. Chem.* **2011,** *76*, 7056-7064.

17. Pristash, S. R.; Corp, K. L.; Rabe, E. J.; Schlenker, C. W., *ACS Applied Energy Materials* **2019**, acsaem.9b01808.

18. Webster, S.; Peceli, D.; Hu, H.; Padilha, L. A.; Przhonska, O. V.; Masunov, A. E.; Gerasov, A. O.; Kachkovski, A. D.; Slominsky, Y. L.; Tolmachev, A. I.; Kurdyukov, V. V.; Viniychuk, O. O.; Barrasso, E.; Lepkowicz, R.; Hagan, D. J.; Van Stryland, E. W., *J. Phys. Chem. Lett.* **2010,** *1*, 2354-2360.

19. Peceli, D.; Hu, H.; Fishman, D. A.; Webster, S.; Przhonska, O. V.; Kurdyukov, V. V.; Slominsky, Y. L.; Tolmachev, A. I.; Kachkovski, A. D.; Gerasov, A. O.; Masunov, A. E.; Hagan, D. J.; Van Stryland, E. W., *J. Phys. Chem. A.* **2013,** *117*, 2333-2346.

20. Huang, L.; Zhao, Y.; Zhang, H.; Huang, K.; Yang, J.; Han, G., *Angew. Chem.* **2017,** *129*, 14592-14596.

21. Pun, J. K. H.; Gallaher, J. K.; Frazer, L.; Prasad, S. K. K.; Dover, C. B.; MacQueen, R. W.; Schmidt, T. W., *Journal of Photonics for Energy* **2018,** *8*, 1.

22. Nishimura, N.; Gray, V.; Allardice, J. R.; Zhang, Z.; Pershin, A.; Beljonne, D.; Rao, A., *ACS Materials Letters* **2019,** *1*, 660-664.

23. Cheng, Y. Y.; Fückel, B.; Khoury, T.; Clady, R. G. C. R.; Ekins-Daukes, N. J.; Crossley, M. J.; Schmidt, T. W., *J. Phys. Chem. A.* **2011,** *115*, 1047-1053.

24. Manna, M. K.; Shokri, S.; Wiederrecht, G. P.; Gosztola, D. J.; Ayitou, A. J.-L., *Chem. Comm.* **2018,** *54*, 5809-5818.

25. Han, J.; Jiang, Y.; Obolda, A.; Duan, P.; Li, F.; Liu, M., *J. Phys. Chem. Lett.* **2017,** *8*, 5865-5870.

26. Gray, V.; Dzebo, D.; Abrahamsson, M.; Albinsson, B.; Moth-Poulsen, K., *Phys. Chem. Chem. Phys.* **2014,** *16*, 10345-10352.

27. Sasaki, Y.; Amemori, S.; Kouno, H.; Yanai, N.; Kimizuka, N., *J. Mater. Chem. C.* **2017,** *5*, 5063-5067.

Chapter 6. Opportunities and challenges for heavy-atom-free photon upconversion systems

6.1 INTRODUCTION

Considering the TTA upconversion mechanism outlined in Chapter 2 (**Figure 2.3**), certain characteristics are required in each molecule of the upconversion system. The sensitizer molecule must have a high triplet yield (Φ_T), a rapid intersystem crossing rate (large k_{isc}), and a triplet lifetime (τ_T) sufficiently long enough to facilitate TTET. The emitter molecules should exhibit fluorescence yields approaching unity, with negligible intersystem crossing. Many polycyclic aromatic hydrocarbons meet the necessary requirements for emitter molecules in TTA upconversion systems, and thus organic molecules have been frequently employed as the fluorescent component of the system. However, it remains a challenge to design fully organic sensitizers for the TTA-UC process, particularly in the visible and NIR region of the solar spectrum. This impediment persists largely because the relationships between electronic structure and intersystem crossing efficiency are multifaceted, with few clear guiding molecular design principles for obtaining heavy-atom-free molecules with near-unity triplet yields *and* desirable absorption properties.[1] The best TTA-UC quantum efficiencies have historically been achieved using transition metal or organometallic triplet sensitizers, whose heavy atom metal centers induce large spin-orbit coupling constants. Many of these organometallic complexes rely on precious metal centers, such as Pt(II), Pd(II), Ir(III), or Ru(II).[2-5] Their precious metals make these sensitizers costly and, in certain cases, toxic,[6] which are potential impediments to industry-scale adoption. Furthermore, these complexes typically rely on metal-to-ligand charge transfer (MLCT) excitations and other comparatively low-oscillator strength transitions that under-utilize

the full potential of organic chromophores.[7-8] Incorporating a heavy metal can be made less expensive by using more earth-abundant materials, such as lead. Semiconducting lead sulfide[9] or selenide[10] quantum dots have been used as triplet sensitizers for upconversion, but the continuum absorption of the quantum dots across the visible ultimately leads to high parasitic losses of the resulting upconverted emission. Some success has been achieved in metal-free triplet sensitizers that incorporate heavy atoms, typically halogens, such as in the case of iodinated BODIPY-derivatives.[6] These organohalide bonds are photolabile and tend to limit the utility of these molecules as upconversion sensitizers.[6] To develop practical heavy-atom-free upconversion systems, it is compelling to identify new strategies for increasing the triplet yield of organic photosensitizers with intense absorption strength in the device-relevant NIR spectral region.

One strategy for developing all-organic, heavy-atom-free photosensitizers involves utilizing nπ* states to enhance intersystem crossing to closely lying ππ* triplet states,[11] as predicted by El-Sayed's Rules. Literature dating back as far as the 1970s[12] has shown that thionating pendant carbonyl groups on various aromatic core structures can open El Sayed-allowed intersystem crossing channels. This strategy has recently been applied to classes of molecules such as perylenediimides,[13] naphthalenediimides,[14] thymines,[15] perinones,[16] and, through our work, on squaraine dyes.[17] Given the facile synthesis and the wide range of accessible derivatives, this thionation approach appears to be a compelling path forward in develop organic, heavy-atom-free sensitizers for TTA upconversion systems.

6.2 Financial scalability assessment of organic sensitizers vs. organometallic counterparts

Implementing heavy-atom-free sensitizers in photon upconversion systems could have a dramatic impact on the overall financial calculus associated with installing a photovoltaic system. For example, consider adding an upconversion system to a 1 km^2 solar farm. The overall cost for such an installation in the U.S. at present would be roughly $40 M.[18] Using a common triplet sensitizer such as platinum octaethylporphyrin (PtOEP,) the cost of material to cover a 1 km^2 solar farm with an optically dense film is approximately $342 M, which is 855% of the cost of the installation. We have recently demonstrated TTA-UC can be sensitized using thionated squaraine molecules.[17] Using a commercially available squaraine molecule, such as squarylium dye III, the cost of material drops to approximately $2.6 M, a mere 6.5% of the total cost of installation and one hundred and thirty times less costly than a platinum-based sensitizer. Squaraine dyes are produced by a similar process to that of indigo dye, using the condensation of an organic acid with an aniline derivative. By analogy to this industrial synthesis of indigo dyes, materials that are produced on global scales of thousands of tons per year, one would anticipate that mass producing easily thionated organic molecules at scale would readily reduce the sensitizer cost for the aforementioned installation to something on the order of $0.2 M. In this case, a significant increase in the theoretical maximum system efficiency (for the sake of argument here, we assume 15% ± 5%, based on spectral matching to the cell's bandgap) could be facilitated by a relatively miniscule increase (roughly 0.5%) in the module cost. To put this assessment another way, successfully implementing a heavy-atom-free upconversion system could help partially offset a portion of the balance of systems cost by providing solar modules with the same nameplate capacity, but at roughly 15% lower prices. According to our rough

analysis, analogous attempts to increase cell efficiency using a precious metal sensitizer would be a cost-prohibitive endeavor.

When one considers pursuing a prospective UC platform, the potential benefits for a particular PV technology should also be borne in mind. The differential improvement that one anticipates obtaining from their UC system will depend in some measure on the optical energy gap of the PV system being used. Relevant practically-achievable efficiency enhancements have been estimated previously by Cahen et al.[19] The overall PV efficiency resulting from the UC and UC + multiple exciton generation (MEG) contributions are plotted in **Figure 1.1** as a function of the cell energy gap. Unsurprisingly, upconverting photons with energies below the bandgap of silicon (E_g = 1.12 eV)[20] could significantly improve the performance of Si solar cells. However, upon careful examination, one soon surmises that upconverting subgap photons for materials with energy gaps on the order of E_g = 1.5 eV could actually produce a greater differential increase in the overall device efficiency than for silicon. One might thus expect upconversion platforms to be first adopted in thin-film technologies with slightly wider bandgaps, such as CdTe (E_g ~1.51 eV, λ_g ~ 820 nm)[21] or perhaps utilized to boost efficiencies in research cell settings for organic and perovskite photovoltaics. Considering the prospective benefit for these alternative PV platforms, it becomes particularly compelling to consider UC systems with the ability to selectively harvest and upconvert NIR photons in the 800 – 1100 nm range.

6.3 KINETIC CONSIDERATIONS IN THE DESIGN OF NIR-ABSORBING TRIPLET SENSITIZERS

With the development of more efficient heavy-atom-free sensitizer molecules, the imperative becomes pushing the absorption of these sensitizers into the NIR. This is necessary to achieve the appropriate spectral match to common photovoltaic materials. Squaraine molecules can be

readily tuned to NIR absorption by synthetically modifying the donor groups flanking the cylcobutadiene core.[22-24] However, as the energy gap of the molecules is reduced, certain kinetic considerations become especially important. This section discusses these kinetic considerations and how they can be used to inform the design of NIR-absorbing thiosquaraine triplet sensitizers.

An inverse relationship exists between the energy gap of a molecule and the rate of non-radiative decay, commonly known as Energy Gap Law, which was laid out by Engelman and Jortner in 1970.[25] Their Energy Gap Law expression can be reduced in the physically practical weak-coupling limit as follows:

$$k_{nr} = \frac{C^2(2\pi)^{1/2}}{\hbar(\hbar\omega_M \Delta E)^{1/2}} exp\left\{-\frac{\Delta E}{\hbar\omega_M}\left[\ln\left(\frac{\Delta E}{d\rho_M}\right) - 1\right]\right\}, \qquad \text{Equation 1.}$$

where C is the effective electronic coupling, ρ_M is the molecular relaxation energy, which Jortner equates to one-half the Stokes shift energy,[25] d represents the number of vibrational modes promoting non-radiative decay (e.g., the vibrational mode responsible for coupling S_0 and S_1), ω_M is the frequency of the related vibration, and ħ is the reduced Planck constant.

The non-radiative decay rate will be in natural competition with the radiative decay rate, k_r, which we estimate using the Strickler-Berg relation,[26] shown below as Eq. 2.

$$k_r = 2303 \times 8\pi c \tilde{\nu}_{ul}^2 n^2 \frac{1}{N}\frac{g_l}{g_u}\int \varepsilon \, d\tilde{\nu}. \qquad \text{Equation 2.}$$

In Eq. 2, c is the speed of light, n is the refractive index, N is Avogadro's number, g_l and g_u are, respectively, degeneracies of l and u. We take representative values of ε to be on the order 10^5 $M^{-1}cm^{-1}$ for thiosquaraines.

As can be seen from Equation 1., Energy Gap Law predicts that k_{nr} will, in the weak coupling limit, exhibit an exponential (actually, superexponential) dependence on the decreasing S_1 energy (ΔE in Eq. 1).[25] The perceived challenge from an applications standpoint (NIR luminescence or imaging, for example) is that, as k_{nr} *speeds up* with decreasing ΔE or S_1, k_f

actually *slows down* (smaller quadratic frequency term in Eq. 2). Thus, non-radiative decay readily outcompetes luminescence. From this loss in emission yield stems the commonly held belief that NIR active photonics based on organic molecular materials are fundamentally incapable of operating with high efficiency. However, in the case of triplet sensitization, the favored contender to compete against k_{nr} is k_{isc}, not k_f., as the overall triplet yield will be described as follows:

$$\Phi_T = \frac{k_{isc}}{k_r + k_{nr} + k_{isc}} \qquad \text{Equation 3.}$$

Thus, as long as k_{isc} remains roughly an order of magnitude faster than k_{nr}, Φ_T remains significant. To estimate reasonably achievable k_{isc} values, we performed ultrafast TA measurements on our prototype TSQ sensitizer. From prior spectroscopic characterization, we know that TSQ exhibits $\Phi_T \sim 1$. Since Φ_T is numerically equal to the product of our measured singlet lifetime (τ_s) and k_{isc}, we can use TA kinetics for TSQ S_1 decay time of $\tau_s = 4.5$ ps (**Figure A-7**) to thus estimate k_{isc}.

Closer inspection of Equation 1 reveals that in addition to the energy gap, the number and frequency of vibrational modes contributing to the nonradiative decay as well as the molecule's Stoke's shift are important factors in determining the overall non-radiative decay rate. These properties are tunable through molecular design. Using typical physical values of these parameters for squaraine dyes, we have evaluated the potential of our thionated squaraine molecules to serve as NIR sensitizers in TTA-UC schemes by estimating the triplet yield through Eq 3. Based on properties for typical squaraine dyes reported in the literature, we can take values as reported in **Table 6.1**.

Table 6.1 Typical values for molecular parameters that contribute to nonradiative decay based on Energy Gap Law

Term	Definition	Typical value
C	Electronic coupling constant	1200 cm^{-1} [25, 27]
d	Number of vibrational modes that induce nonradiative transition	1 [27]
$\hbar\omega_M$	frequency of the promoting vibrational modes	1300 cm^{-1} [28]
ρ_M	Molecular nuclear relaxation energy	25 – 200 meV [29]

6.4 KINETIC ANALYSIS OF THE TRIPLET YIELD IN THIOSQUARAINES

Our initial assessment indicates that NIR-absorbing thiosquaraines are a compelling testbed for understanding structure-activity relationships needed to achieve high Φ_T values with NIR heavy-atom-free sensitizers. **Figure 6.1** depicts our preliminary kinetic modeling of Φ_T (Eqs. 1 - 3) for thiosquaraines based on Energy Gap Law.[25] The contour that is shaded here in red indicates that, even for thiosquaraines that absorb strongly within our targeted 800 nm – 1200 nm spectral region, Φ_T values approaching unity should still be achievable.

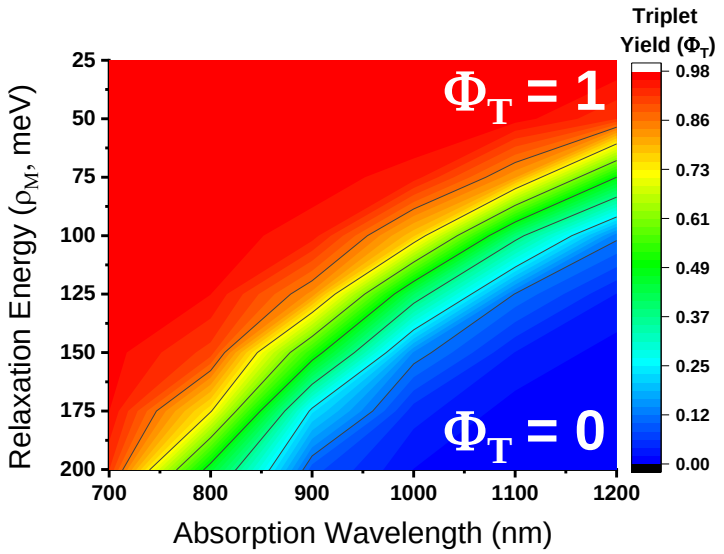

Figure 6.1. Our Energy Gap Law modeling (Eqs. 1 – 3) indicates that unique photophysics of NIR-absorbing thiosquaraines that we will develop allow them to achieve remarkably high triplet yields (Φ_T = 1), despite perceptions that NIR organic photonics cannot operate efficiently due to fast non-radiative decay.

6.5 Additional Considerations for Squaraines in Upconversion-Assisted Photovoltaics

We hypothesize that the sharp absorption lineshapes characteristic of squaraines actually make them ideal candidates for upconversion-assisted photovoltaics. This is somewhat counterintuitive, as it is tempting to assume a single sensitizer with broadband spectral coverage would be desirable for harvesting subgap NIR solar photons. This perception may perhaps be one reason why squaraines and related dyes had not been investigated for UC prior to our work. However, we arrived at a contradictory conclusion. In our assessment, the challenge of upconverting a spectrally broad swath of NIR photons using a TTA-UC platform will ultimately be most readily surmounted using multiple complementary sensitizers, each with a relatively *narrow* absorption linewidth. We rationalize this based on the several considerations outlined below.

One appealing characteristic of narrow-band NIR sensitizers is that the lineshape minimizes parasitic spectral overlap between the sensitizer and the emitter. Minimal parasitic overlap prevents the dyes from reabsorbing outgoing upconverted light, while collecting incoming NIR. Reabsorption decreases efficiency. By contrast, the absorptive and emissive components demonstrate significant overlap with many other common UC sensitizers. Porphyrins, for example, which are possibly one of the most ubiquitously studied UC sensitizers, exhibit intense Soret absorption bands in the visible region of the spectrum. The molar absorptivities (ε) of the lower-energy NIR absorbing Q-band transitions are, at best, roughly equivalent to or, more commonly, at least an order of magnitude smaller than ε for the higher-energy Soret bands. Excessive parasitic absorption of UC light is the common result.

The narrow absorption bands of thiosquaraine sensitizers could perhaps best be utilized in a composite solar UC film containing rubbery polymer nanoparticles or microdroplets, represented pictorially in **Figure 6.2**. A film architecture is ideal for facile integration into a photovoltaic device, and in Chapter 4 we demonstrate that the TSQ/rubrene system exhibits upconversion in a rubbery polymer film. In the example in **Figure 6.2**, each particle in the UC film is enriched with the same type of emitter, with S_1 energy above the bandgap of the solar cell, 600 nm for example. Each also contains one type of sensitizer molecule from a series, where each exhibit one single narrow NIR absorption band centered at either, 800 nm, 900 nm, 1000 nm, 1100 nm, etc. TTET from each sensitizer to the emitter is exergonic. An optically-dense UC layer of this composite of particles would absorb a broad band of NIR light but exhibit a single UC emission peak at 600 nm. To avoid parasitic absorption of this upconverted emission, each dye would ideally exhibit only a narrow NIR absorption peak and nearly-zero absorption in the visible

region. The example that we show in **Figure 6.2** demonstrates that such an absorption profile will be readily achievable with squaraine-like dyes.

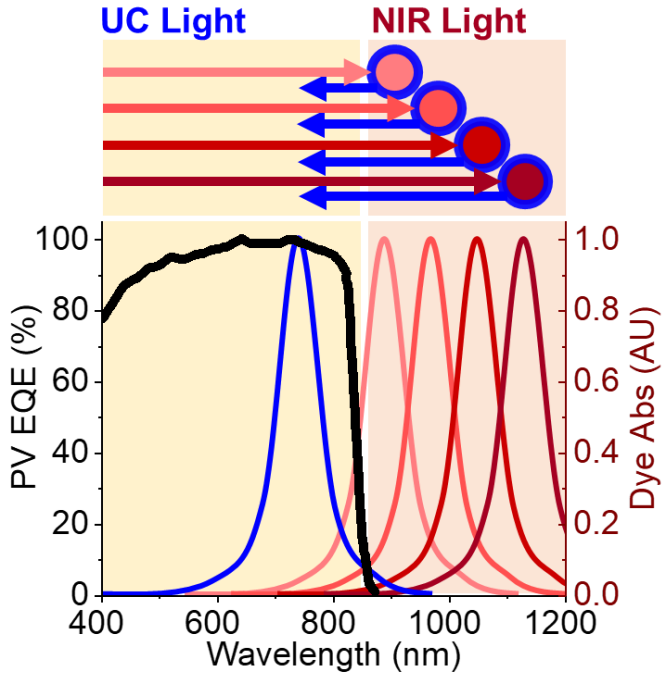

Figure 6.2. Schematic of cooperative NIR sensitizer composites with a common emitter, paired with a photovoltaic device. We hypothesize that the narrow-band absorption of thionated squaraine-like dyes is an advantage over broadband sensitizers for NIR UC: 1) The sensitizers won't strongly absorb emitted UC light; 2) Narrow line widths mean that photons at shorter NIR wavelengths produce sensitizer states with longer lifetimes than in a single broad-band absorber. CdTe EQE data reproduced from reference [30].[30]

The modularity of harvesting narrow slices of the NIR spectrum with multiples dyes (**Figure 6.2**) may also help to decouple competing performance requirements. For example, achieving efficient Φ_T can be partially decoupled from achieving NIR-absorption. Achieving efficient Φ_T is governed by obtaining rapid k_{isc} to outcompete the exponentially increasing k_{nr} as the S_1 energy decreases, relative to S_0. Due to fast vibronic relaxation to S_1 and rapid k_{nr} from S_1, a single dye, absorbing strongly over a wide spectral range, will tend to indiscriminately funnel the energy of all of these photons to its lowest energy S_1 excited state. Thus, photons on the higher-energy side of the absorption band produce excited states that must compete against the same fast k_{nr} as those

from photons on the lower-energy edge. Dividing the task of absorption among multiple narrow-band dyes will produce a distribution of slower k_{nr} values, which should lead to an increase in the overall triplet yield. That is, perhaps ISC time constants of ~5 ps are fine for absorbing 800 nm – 1050 nm photons. However, a significant molecular engineering effort may be required for designing sensitizers in the 1050 nm – 1200 nm range to ensure that k_{isc} outcompetes k_{nr}.

An analogous rate constant argument could be made for maximizing T_1 lifetimes of a series of NIR dyes. In contrast to a single broadband absorber, a modular approach, with multiple narrow-band sensitizers to split the workload, could help maximize the available time for TTET to an emitter. By contrast, for a single broadband NIR sensitizer, all photons yield sensitizer triplets with a common faster time constant.

6.6 CONCLUSIONS

Photon upconversion shows immense promise to improve a number of photovoltaic and biological applications. Triplet-triplet annihilation upconversion is an attractive mechanism due to its low incident power requirements and the high tunability of excitation and emission wavelengths. Replacing commonly used precious metal complexes with organic sensitizers in TTA-UC systems could dramatically reduce the cost and thus the barriers to scalability for these systems. In this chapter, we discuss thionation as a synthetically simple methodology of increasing intersystem crossing yields, producing triplet states efficiently on organic molecules without the use of heavy atoms. This strategy is highly appealing in the future development of all-organic upconversion systems. Additionally, our kinetic evaluation shows that the thiosquaraine platform shows promise to exhibit high triplet yields even at low energy gaps, allowing for the design of spectrally relevant NIR absorbing materials for photovoltaic applications.

6.7 REFERENCES

1. Zhao, J.; Chen, K.; Hou, Y.; Che, Y.; Liu, L.; Jia, D., *Org. Biomol. Chem.* **2018,** *16*, 3692-3701.

2. Singh-Rachford, T. N.; Castellano, F. N., *Coord. Chem. Rev.* **2010,** *254*, 2560-2573.

3. Cui, X.; Zhao, J.; Yang, P.; Sun, J., *Chem. Comm.* **2013,** *49*, 10221-10223.

4. Castellano, F. N.; Singh-Rachford, T. N., *J. Phys. Chem. A.* **2008,** *112* (16), 3550-3556.

5. Kimizuka, P. D.; Nobuhiro, Y.; Nobuo, *Chem. Comm.* **2014,** *50*, 13111-13113.

6. Wu, W.; Guo, H.; Wu, W.; Ji, S.; Zhao, J., *J. Org. Chem.* **2011,** *76*, 7056-7064.

7. Ji, S.; Guo, H.; Wu, W.; Wu, W.; Zhao, J., *Angew. Chem. Int. Ed.* **2011,** *50*, 8283-8286.

8. Islangulov, R. R.; Castellano, F. N., *Angew. Chem. Int. Ed.* **2006,** *45*, 5957-5959.

9. Nishimura, N.; Allardice, J. R.; Xiao, J.; Gu, Q.; Gray, V.; Rao, A., *Chem. Sci.* **2019,** *10*, 4750-4760.

10. Huang, Z.; Li, X.; Mahboub, M.; Hanson, K. M.; Nichols, V. M.; Le, H.; Tang, M. L.; Bardeen, C. J., *Nano Lett.* **2015,** *15*, 5552-5557.

11. Castellano, T. N. S.-R.; Felix, N., *J. Phys. Chem. A.* **2009,** *113* (20), 5912-5917.

12. Anderson, R. W.; Hochstrasser, R. M.; Pownall, H. J., *Chemical Physics Letters* **1976,** *43*, 224-227.

13. Tilley, A. J.; Pensack, R. D.; Lee, T. S.; Djukic, B.; Scholes, G. D.; Seferos, D. S., *J. Phys. Chem. C.* **2014,** *118*, 9996-10004.

14. Hussain, M.; Zhao, J.; Yang, W.; Zhong, F.; Karatay, A.; Yaglioglu, H. G.; Yildiz, E. A.; Hayvali, M., *J. Lumin.* **2017,** *192*, 211-217.

15. Pollum, M.; Jockusch, S.; Crespo-Hernández, C. E., *J. Am. Chem. Soc.* **2014,** *136*, 17930-17933.

16. Palmer, J. R.; Wells, K. A.; Yarnell, J. E.; Favale, J. M.; Castellano, F. N., *The Journal of Physical Chemistry Letters* **2020,** *11*, 5092-5099.

17. Pristash, S. R.; Corp, K. L.; Rabe, E. J.; Schlenker, C. W., *ACS Applied Energy Materials* **2019**, acsaem.9b01808.

18. Davis, M.; White, B.; Goldstein, R.; Martinez, S. L.; Chopra, S.; Goss, K.; Sahd, M.; Sun, X.; Rumery, S.; Silver, C.; Baca, J. *US Solar Market Insights*; Wood Mackenzie/Solar Energy Industries Association: 2021.

19. Shpaisman, H.; Niitsoo, O.; Lubomirsky, I.; Cahen, D., *Sol. Energy Mater. Sol. Cells* **2008,** *92*, 1541-1546.

20. Neamen, D. A., *Semiconductor Physics and Devices. Third ed*. McGraw-Hill: 2003.

21. Fonthal, G.; Tirado-Mejía, L.; Marín-Hurtado, J. I.; Ariza-Calderón, H.; Mendoza-Alvarez, J. G., *J. Phys. Chem. Solids* **2000,** *61*, 579-583.

22. Chen, G.; Sasabe, H.; Igarashi, T.; Hong, Z.; Kido, J., **2015,** *3*, 14517-14534.

23. Strassel, K.; Kaiser, A.; Jenatsch, S.; Véron, A. C.; Anantharaman, S. B.; Hack, E.; Diethelm, M.; Nüesch, F.; Aderne, R.; Legnani, C.; Yakunin, S.; Cremona, M.; Hany, R., *ACS Appl. Mater. Interfaces* **2018,** *10*, 11063-11069.

24. Suresh Regional Research Lab, V.; Council of, S.; Industrial Research Csir, S. R. R. L. D. A. S.; Kakkudiyil, G. R. R. L. T.; Biju Vasudevan Regional Res. Lab, P.; Santosh Regional Research Lab, U. Squaraine based dyes and process for preparation thereof. 2003-09-03, 2003.

25. Englman, R.; Jortner, J., *Mol. Phys.* **1970,** *18* (2), 145-164.

26. Strickler, S. J.; Berg, R. A., *The Journal of Chemical Physics* **1962,** *37*, 814-822.

27. Wei, Y. C.; Wang, S. F.; Hu, Y.; Liao, L. S.; Chen, D. G.; Chang, K. H.; Wang, C. W.; Liu, S. H.; Chan, W. H.; Liao, J. L.; Hung, W. Y.; Wang, T. H.; Chen, P. T.; Hsu, H. F.; Chi, Y.; Chou, P. T., *Nature Photonics* **2020,** *14*, 570-577.

28. Hestand, N. J.; Zheng, C.; Penmetcha, A. R.; Cona, B.; Cody, J. A.; Spano, F. C.; Collison, C. J., *J. Phys. Chem. C.* **2015,** *119*, 18964-18974.

29. McNamara, L. E.; Rill, T. A.; Huckaba, A. J.; Ganeshraj, V.; Gayton, J.; Nelson, R. A.; Sharpe, E. A.; Dass, A.; Hammer, N. I.; Delcamp, J. H., *Chemistry – A European Journal* **2017,** *23*, 12494-12501.

30. Wu, X., *Solar Energy* **2004,** *77*, 803-814.

APPENDIX A: SUPPLEMENTARY INFORMATION FOR CHAPTER 4

Figure A-1a shows the evolution-associated decay spectra (EADS) associated with the thiosquaraine triplet. The EADS are identical both in the case with and without rubrene, showing that the thiosquaraine is spectrally resolvable and giving credence to the assignment of the new spectral feature as the rubrene triplet shown in **Figure 4.6d** of the main text. **Figure A-1b** shows the extracted kinetics traces from the global analysis fits, which are in agreement with the data shown in **Figure 4.6c** of the main text. These fits show that the thiosquaraine triplet lifetime is significantly quenched in the presence of rubrene.

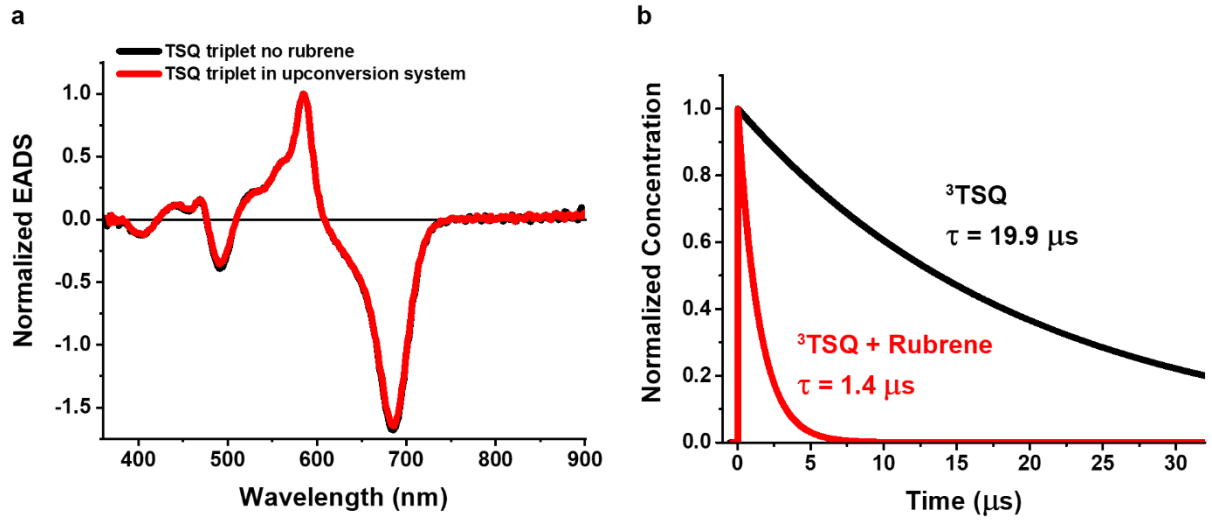

Figure A-1. (a) Thiosquaraine triplet component extracted from global analysis from both datasets with and without rubrene. The triplet components are identical, regardless of the presence of rubrene. (b) Global *A*nalysis fits of the thiosquaraine triplet absorption both with and without the presence of rubrene, showing the dynamic quenching of the thiosquaraine triplet state when rubrene is present.

Figure A-2 shows frequency modulation dependence data of the thiosquaraine triplet as monitored in the quasi-steady state method of photoinduced absorption. For this data, the probe wavelength is set to 585 nm and the modulation frequency of the 685 nm pump is varied. The monitored photoinduced absorption signal should have a flat response until the modulation frequency becomes too fast for the population of photoexcited chromophores to decay within the modulation cycle of the optical excitation. At this point the amplitude of the PIA signal diminishes with increasing modulation frequency. Thus, spectral features with a longer lifetime will exhibit a roll-off behavior at lower frequencies than those with shorter lifetimes. **Figure A-3** shows that the frequency role-off occurs at lower frequencies for the isolated thiosquaraine than for thiosquaraine in the presence of rubrene, suggesting that the presence of rubrene shortens the lifetime of the thiosquaraine triplet.

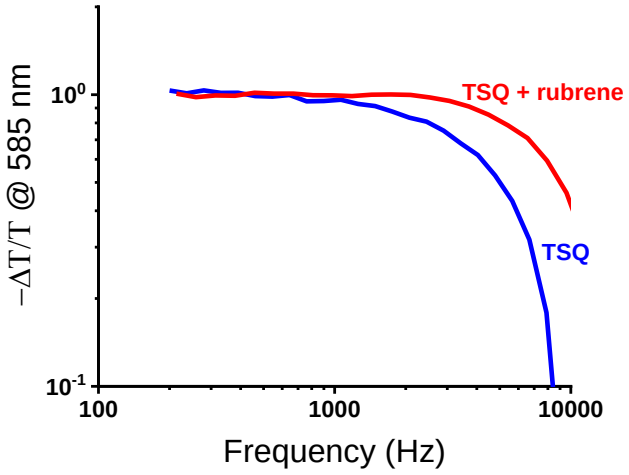

Figure A-2. Frequency modulation dependence of the thiosquaraine triplet absorption, monitored with a probe wavelength 585 nm. As the frequency of the photomodulation increases, a drop off in signal is expected. This drop off happens at lower frequencies for species that have longer lifetimes. When in the presence of rubrene, the frequency response is flattened with respect to the native thiosquaraine triplet response, suggesting a shorter lifetime in the presence of rubrene.

Figure A-3a shows the ^{3}TSQ induced absorption signal for the isolated thiosquaraine chromophore in toluene, with no rubrene added, monitored at a probe wavelength of 585 nm over a period of at least 10 hours of pump illumination. The intensity of the ^{3}TSQ photoinduced absorption signal is unchanged over this extended period, demonstrating the intrinsic photostability of the molecule in deaerated solution. This is in contrast to a number of iodo-BODIPY sensitizers, which have been shown to bleach over the course of a few hours of illumination. A similar experiment is shown for the upconverted photoluminescence in **Figure A-3b**, demonstrating that the upconverted fluorescence is stable over at least 35 hours.

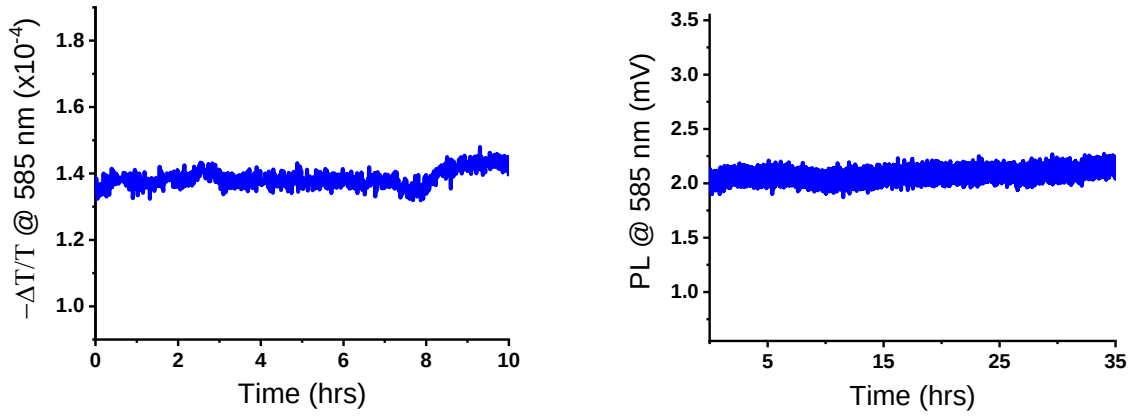

Figure A-3. Single wavelength over time monitoring of (a) the ^{3}TSQ induced absorption signal of the isolated ^{3}TSQ at 585 nm and (b) the upconverted fluorescence signal detected at 585 nm showing that these signals do not lose intensity over a period of 10 or 35 hours, respectively.

Figure A-4a shows the absorbance and emission of the thiosquaraine in a glassy 2-methyl-THF matrix at 80K. The kinetics of the emission are shown in **Figure A-4b**. The lifetime of this emission is 3.5 ns. The short lifetime, along with the small Stokes shift, suggests that emission is from the singlet state.

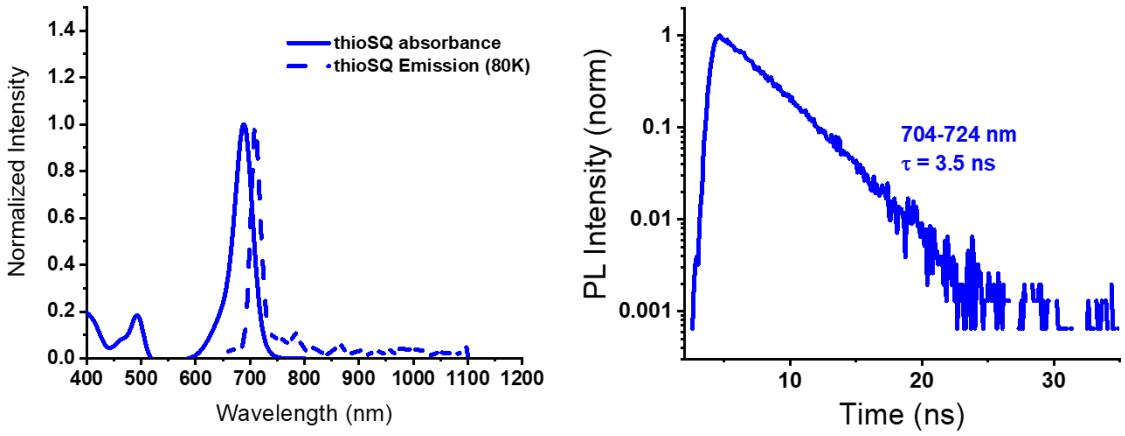

Figure A-4. (a) Absorbance and photoluminescence of thiosquaraine at 80K, where fluorescence is observed. (b) Kinetics of the thiosquaraine emission at 80K, showing a 3.5 ns lifetime.

Figure A-5 and **Figure A-6** show the ^{1}H-NMR spectra of the thiosquaraine and parent squaraine after purification, used as confirmation of the chemical structures.

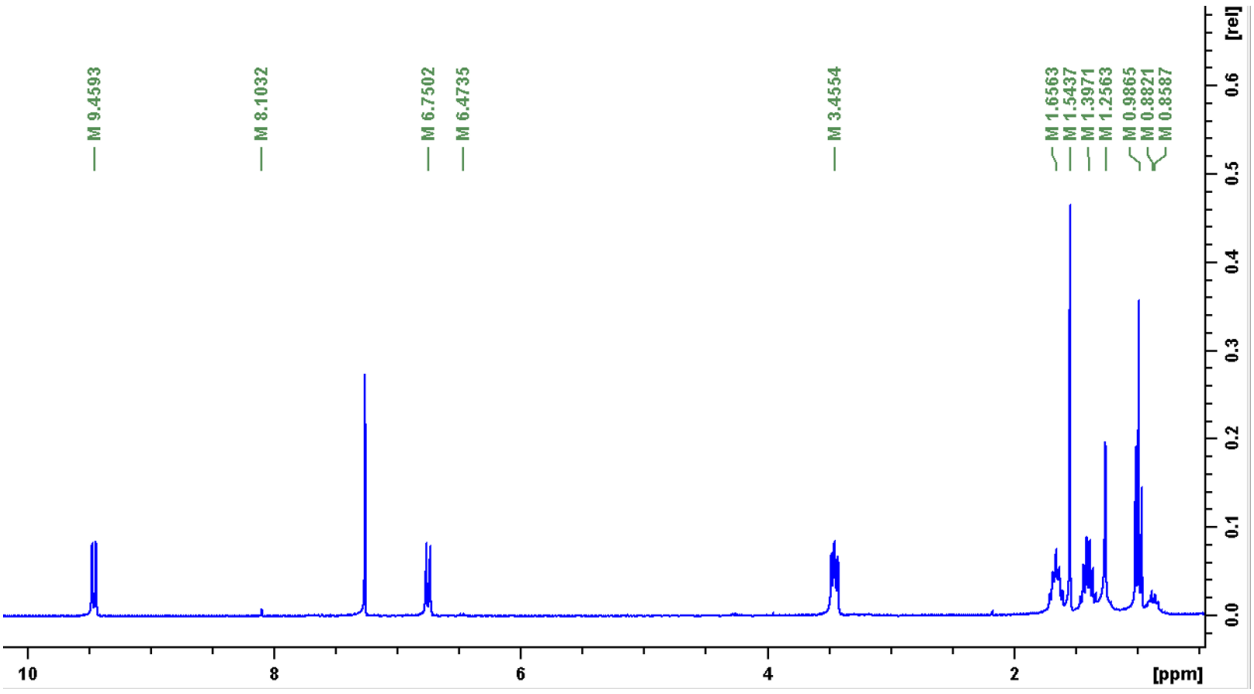

Figure A-5. ^{1}H-NMR spectrum of thiosquaraine after purification

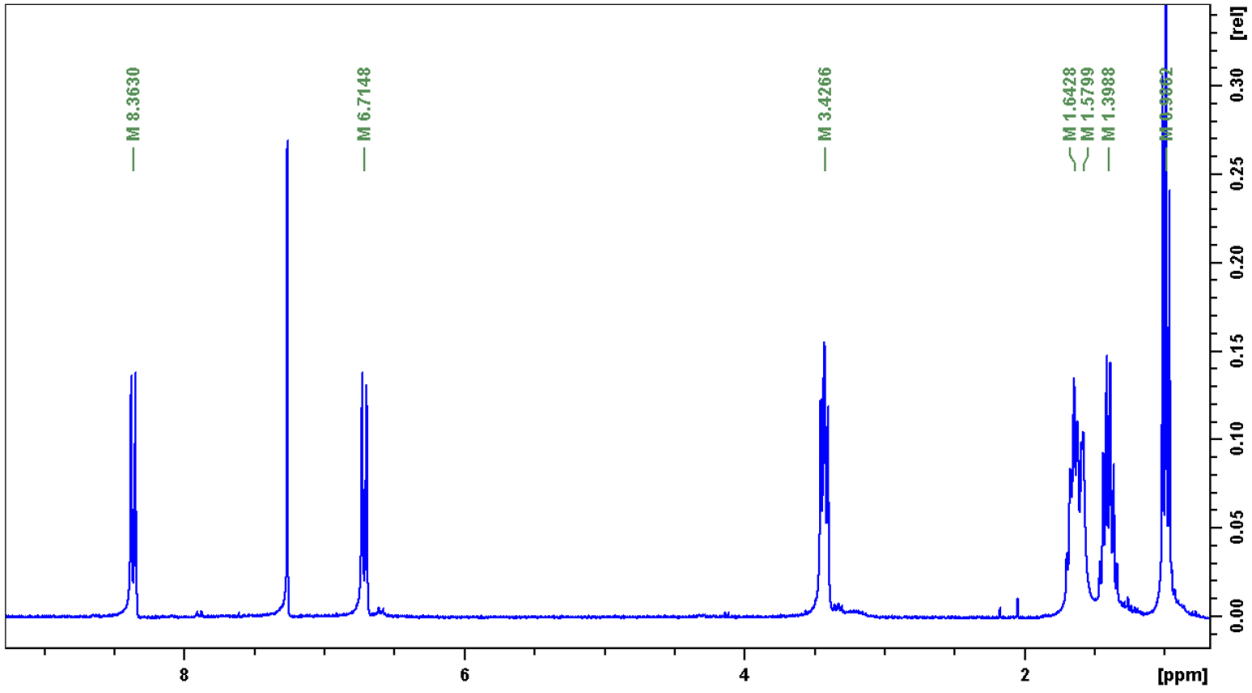

Figure A-6. ^{1}H-NMR spectrum of parent squaraine after purification

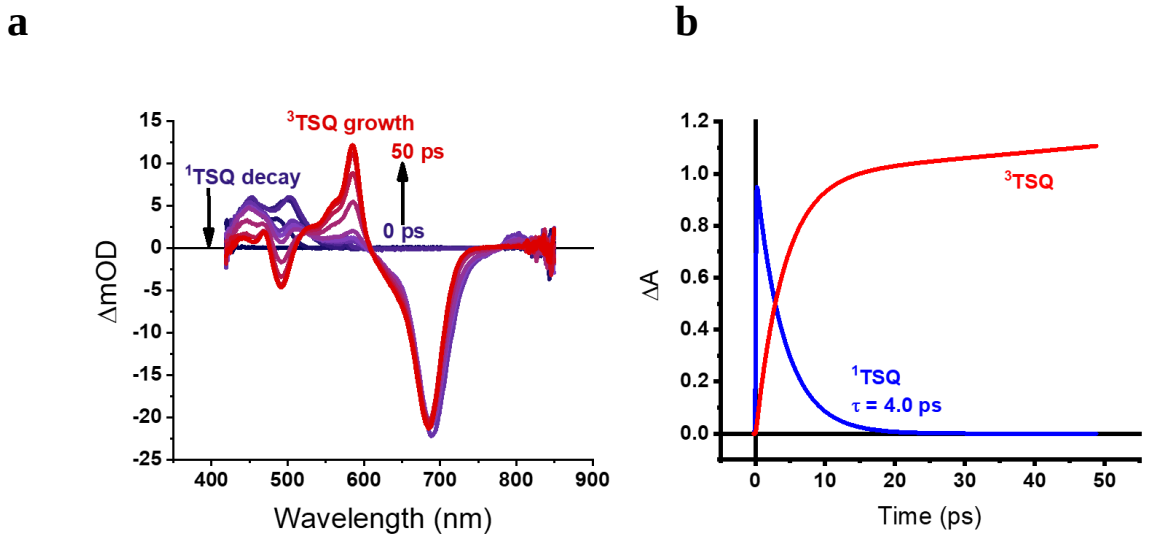

Figure A-7. Picosecond-scale transient absorption data showing the kinetics of intersystem crossing in TSQ. Figure (a) shows the spectral evolution over the first 50 picoseconds while (b) shows the kinetics of the features associated with the TSQ singlet (~450 nm) and the TSQ triplet (~590 nm).

APPENDIX B: SUPPLEMENTARY INFORMATION FOR CHAPTER 5

Figure B-1 shows the upconverted emission spectrum of the TSQ/TiPS-An solution under 730 nm excitation. This demonstrates that upconversion can be driven on the red edge of the TSQ absorption. The excitation source is a 730 nm laser diode purchased from RPMC lasers, product number HL7301MG, driven by a Keithley 2400 sourcemeter.

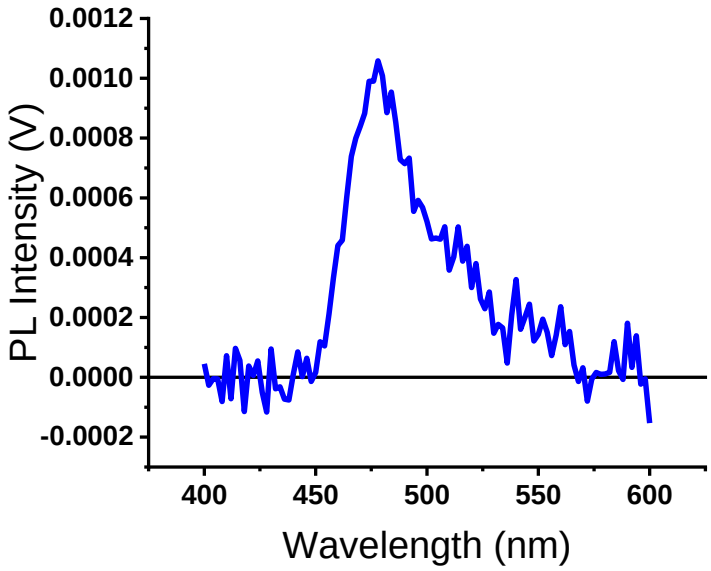

Figure B-1. Upconverted fluorescence from TiPS-Anthracene by 730 nm excitation of the thiosquaraine sensitizer. This is one of the few reported examples of >700 nm excitation resulting in <500 nm emission in any upconversion system.[1-2]

Upconversion Lifetime measurement:

In our previous reported upconversion system, the upconversion emission lifetime was measured using a Hamamatsu streak camera (C10910) with a slow-sweep unit (M10913-01). Samples were

irradiated with the 700 nm output of a Coherent/Light Conversion OPerA Solo OPA that was pumped with 50 fs pulses from a 1 kHz Ti:sapphire amplifier (Libra-HE, Coherent) with an average incident photon density of 1.4×10^{14} photons/cm^2/pulse. With this excitation density, no emission was seen from a control sample of just rubrene. However, due to the efficiency limits of the TSQ/TiPS-An system, higher excitation densities were needed and as such we were unable to measure upconverted emission without also observing a kinetic signature of native TiPS-An emission populated through two-photon absorption. **Figure B-2** demonstrates this limitation. Here, the laser pulses are compressed in time such that the while the average incident power density is low, the peak power intensity is large enough to induce a two-photon absorption effect.

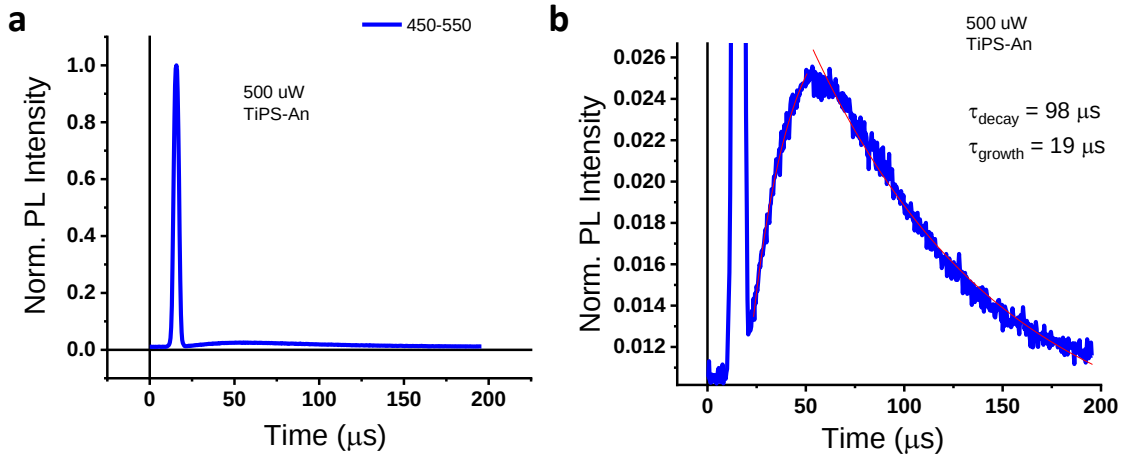

Figure B-2. (a) Upconverted fluorescence from TiPS-Anthracene by 700 nm excitation of the thiosquaraine sensitizer on the time-resolved photoluminescence system. A high intensity emission with a short lifetime is observable resulting from two-photon absorption, and a lower intensity signal is visible over a longer timescale. (b) An enlarged view of the upconverted emission signal. Interestingly, the rise time of the upconverted emission signal is 19 μs, which is consistent with the TSQ triplet lifetime.

To get around this issue of high peak powers for our fs-pulsed laser system, the upconverted emission kinetics were measured with a 685 laser diode modulated by a function generator. The

frequency of the modulation was set so that the period was significantly longer than the upconversion lifetime, and the kinetics were measured off the falling edge of the resulting square wave. Scattered excitation light was measured as an instrument response function, and the resulting lifetime was determined by fitting the decay kinetics to a two component exponential decay, with the first component set to the decay time of the IRF. This data is shown in **Figure B-3**.

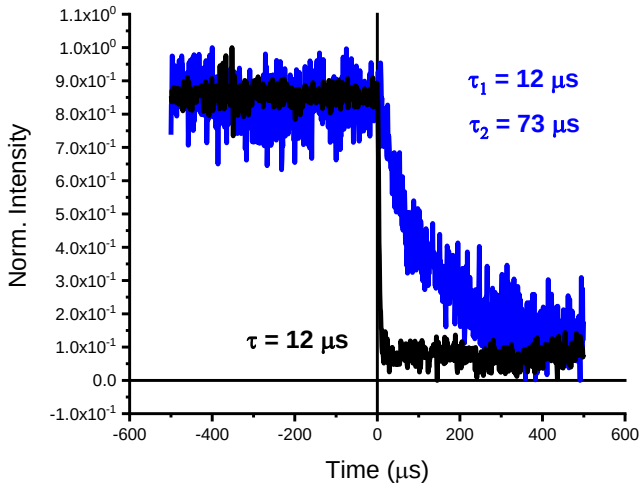

Figure B-3. The measured IRF (black) and decay kinetics (blue) of the TSQ/TiPS-An upconversion system. The lifetime of the upconversion was determined by fitting the decay of the IRF and then fixing that as the first component of a two-component decay for the upconverted emission. The second component of that fit is reported as the upconverted emission lifetime.

Temperature dependence of TiPS-An emission:

Figure B-4 demonstrates that over the temperature range used in this study, the TiPS-An native fluorescence is not temperature dependent. This serves as a control to verify that the temperature dependence observed in the upconverted emission is not an artifact of the emitter.

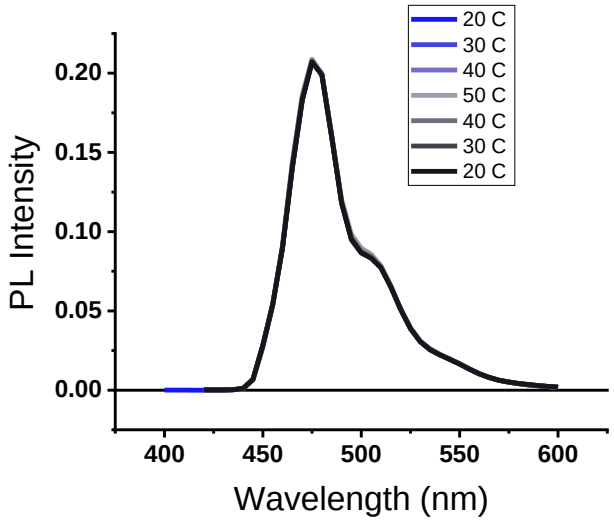

Figure B-4. Temperature dependence of the native TiPS-An fluorescence excited at 365 nm. The emission shows no change in intensity over an increase from 20 ºC to 50 ºC or the following decrease from 50 ºC back to 20 ºC

Figure B-5 further demonstrates that we see the opposite trend in the TSQ/rubrene system than the TSQ/TiPS-An system, with a decrease in emission intensity as the temperature is increased.

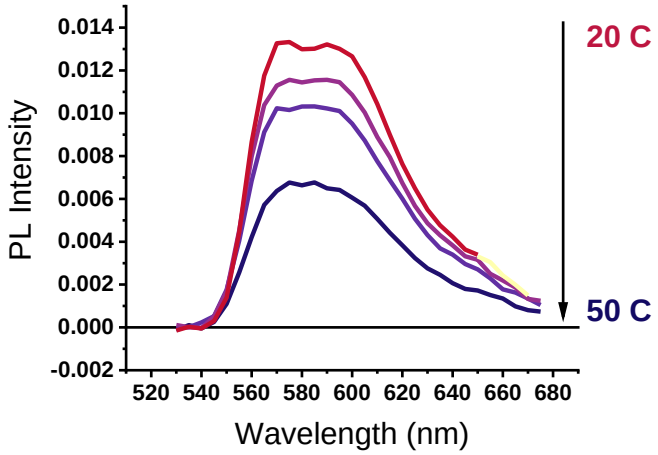

Figure B-5. Temperature dependent luminescence traces for the TSQ/Rubrene upconversion system. This system shows opposite behavior from the TSQ/TiPS-An. As the temperature increases from 20˚C to 50˚C, the luminescence intensity decreases.

TSQ/1CBEPA upconverted emission:

Figure B-6 shows the upconverted emission of the TSQ/1CBPEA system. No emission is observed unless both components are present in solution, and the upconverted emission is spectrally identical to that of the native 1CBPEA fluorescence.

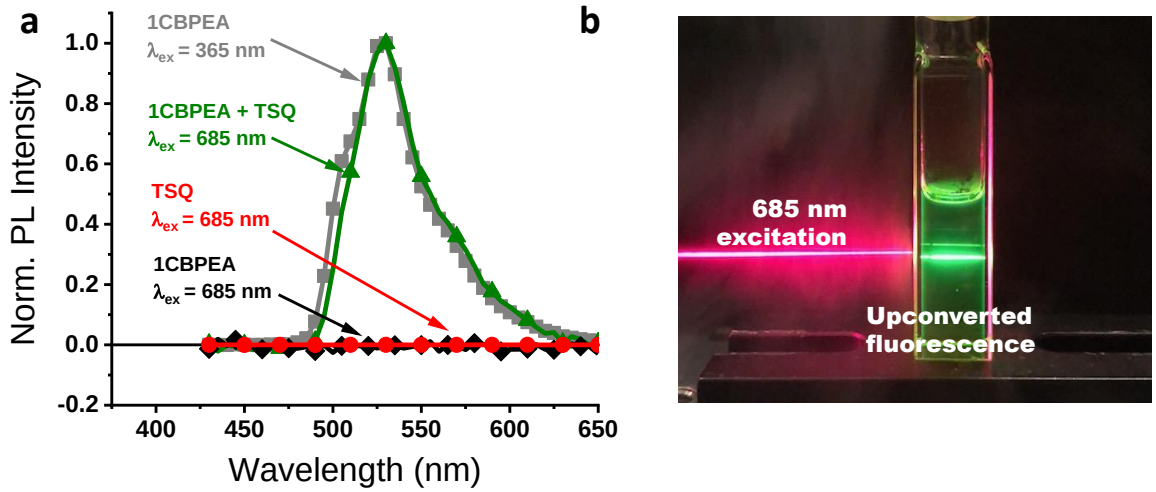

Figure B-6. (a) Selective excitation of the thiosquaraine at 685 nm leads to upconverted fluorescence from the 1CBPEA component. This fluorescence is identical to the fluorescence observed when 1CBPEA is excited at 365 nm. No fluorescence is observed from either individual molecule when excited in isolation at λex = 685 nm. (b) Photograph of upconverted emission resulting from 685 nm excitation.

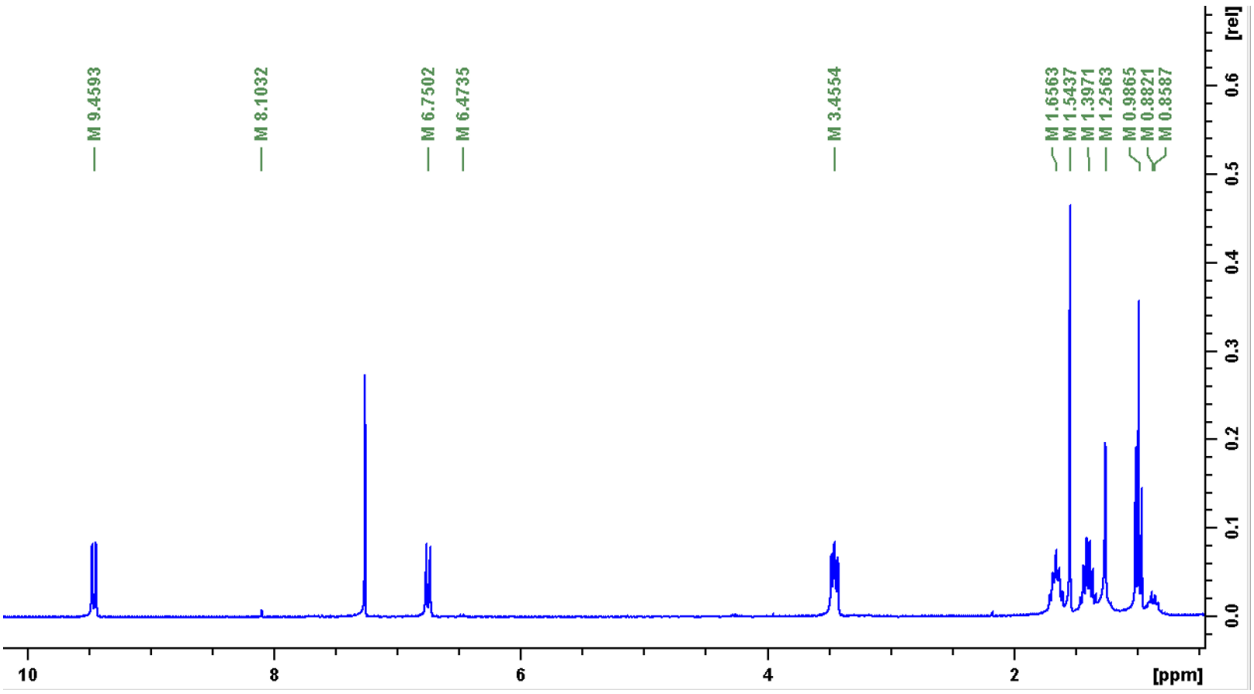

Figure B-7. [1]H-NMR spectrum of thiosquaraine after purification

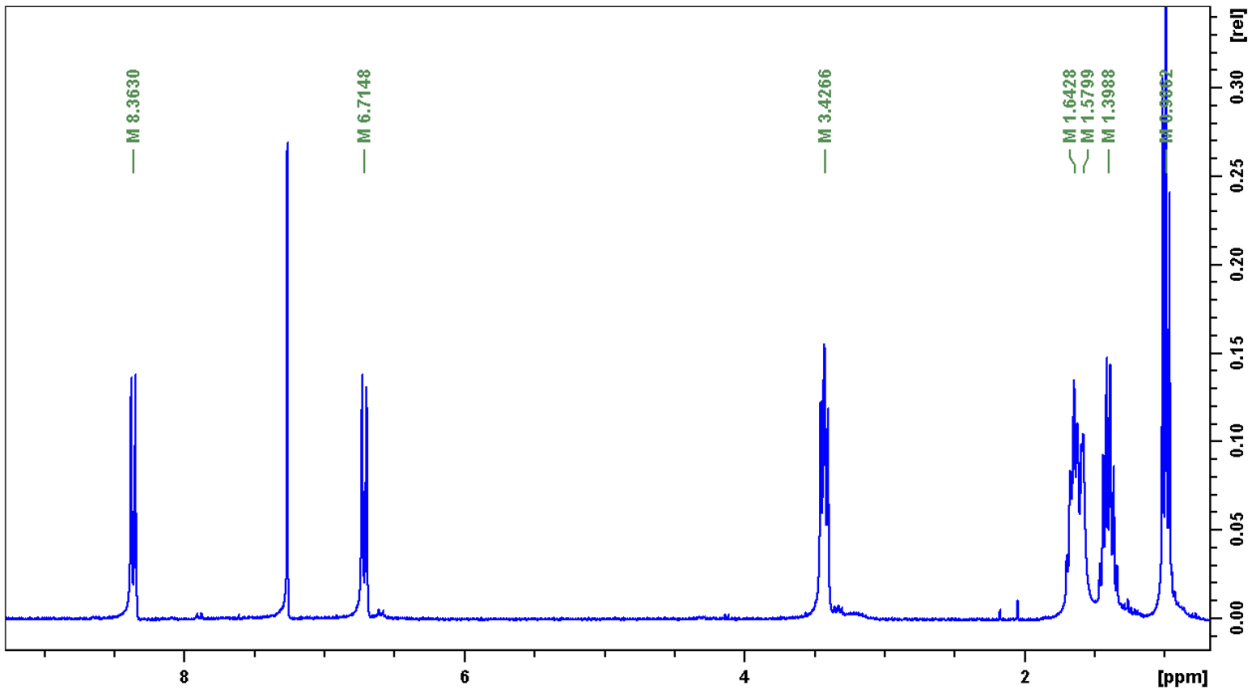

Figure B-8. [1]H-NMR spectrum of parent squaraine after purification

References:

1. Sasaki, Y.; Amemori, S.; Kouno, H.; Yanai, N.; Kimizuka, N., *J. Mater. Chem. C.* **2017,** *5*, 5063-5067.

2. Bharmoria, P.; Bildirir, H.; Moth-Poulsen, K., *Chem. Soc. Rev.* **2020,** *49*.

VITA

Sarah Pristash

802 N 43rd St, Apt 102, Seattle WA 98103
(607) 591-6315 • spristash3@gmail.com
https://www.linkedin.com/in/spristash/

Qualifications

- Experience with Python for data analysis and visualization as well as software engineering. Relevant libraries include Pandas, Numpy, SciKitLearn, GeoPandas, Tensorflow
- Enhanced laboratory skills through research assistant positions in multiple chemistry labs.
- Research, data collection, analytical, and writing skills developed in natural science courses.
- Strong interest in green chemistry, pollution, and renewable energy.
- Experience with various instruments and methods used in scientific research.
    - Familiarity with various spectroscopic methods including UV/Vis, fluorometry, FTIR, lock-in detected absorption and luminescence, transient absorption
- Strong organizational, planning and leadership skills developed through leadership positions in campus extracurriculars.
- Experience with Microsoft Word, Powerpoint, Excel, IGOR Pro, LabView, and OriginLab for data collection and presentation

Chemistry Education

University of Rochester **Rochester, NY**
Bachelor of Science in Chemistry *May 15, 2016*

- Department Denoted "Highest Distinction"
- University Denoted *Cum Laude*
- Cumulative GPA: 3.76
- Major GPA: 3.78
- Dean's List 6 of 8 completed semesters
- Teaching assistantships:
  Organic Chemistry I&II – 2014-2015 school year, 2015-2016. *Responsibilities include teaching a weekly workshop and training new teaching assistants.*
  Physical Chemistry I&II (Quantum Chemistry and Molecular Thermodynamics) – 2015-2016 school year. *Responsibilities include teaching a weekly workshop, grading homework assignments, and hosting a weekly office hour.*

University of Washington **Seattle, WA**
Graduate Studies, Ph.D. *March 2022*

- Cumulative GPA: 3.77
- Awarded National Science Foundation Graduate Research Fellowship

Awards and Honors

- National Science Foundation Graduate Research Fellowship
  The NSF Graduate Research Fellowship Program recognizes and supports outstanding graduate students in NSF-supported science, technology, engineering, and mathematics disciplines who are pursuing research-based Master's and doctoral degrees at accredited United States institutions

- Data Intensive Research Enabling Clean Technologies (DIRECT) Fellow, Clean Energy Institute
  DIRECT trains the next generation of young scientists and engineers to apply modern data science tools to the traditional aspects of materials design, synthesis, and characterization
- Mark Torrance Foundation Policy Analyst – CEI Advanced Experience Program
  The Advanced Experience Program (AXP), created through the generous support of the Mark Torrance Foundation, will enable UW doctoral students in science, technology, engineering, and mathematics (STEM) to apply their knowledge to support decision makers in cleantech investing and clean energy policy.
- Junior Scholar Award at University of Rochester
  Given to chemistry students in the junior class, in recognition of outstanding accomplishment and promise for a professional career in chemistry.
- ACS Outstanding Achievement in Chemistry, Rochester Section Award
  This award is given to a senior with an outstanding academic record and includes recognition at the ACS Annual Rochester Section Undergraduate Research Symposium.
- Carl J. Whiteman, Jr. Teaching Award
  This award recognizes exemplary teaching by an undergraduate student in the Department of Chemistry.
- Awarded New York State Excellence and Dean's Scholarship at University of Rochester

Publications

Heavy-Atom Free Red-to-Yellow Photon Upconversion in a Thiosquaraine Composite
Pristash, S.R.; Corp, K.L.; Rabe, E.J.; Schlenker, C.W., *ACS Appl. Energy Mater*. **2020**, *3*, 1, 19-28

Singlet-Triplet Inversion in Heptazine and in Polymeric Carbon Nitrides
Ehrmaier, J.; Rabe, E.J.; Pristash, S.R.; Corp, K.L.; Schlenker, C.W.; Sobolewski, A.L.; Domcke, W., *J. Phys. Chem. A.*, **2019**, *123*, 38, 8099-8108

Phase separation, crystallinity and monomer-aggregate population control in solution processed small molecule solar cells
Zheng, C.; Bleier, D.; Jalan, I.; Pristash, S.; Penmetcha, A. R.; Hestand, N. J.; Spano, F. C.; Pierce, M. S.; Cody, J. A.; Collison, C. J. *Sol. Energy Mater. Sol. Cells* **2016**, *157*, 366–376.

Patents

US Provisional Patent, serial number 63/083,499 filed 9/25/2020
"HEAVY-ATOM FREE SENSITIZERS FOR TRIPLET-TRIPLET ANNIHILATION UPCONVERSION SYSTEMS"

International PCT Patent Application, PCT/US2021/051467 filed 9/22/2021
"HEAVY-ATOM FREE SENSITIZERS FOR TRIPLET-TRIPLET ANNIHILATION UPCONVERSION SYSTEMS"

Presentations

International Conference on Energy Conversion and Storage (ORCAS) – 2020
Poster presentation, *"Heavy-atom-free Photon Upconversion Using Thionated Organic Sensitizers"*

ACS Northwest Regional Meeting (NORM) – 2021
Oral presentation, *"Heavy-atom-free triplet-triplet annihilation upconversion with a thiosquaraine sensitizer"*

NanoEngineering and Sciences Seminar, UW - 2021
Oral presentation, *"Heavy-atom-free triplet-triplet annihilation upconversion with a thiosquaraine sensitizer"*

Chemistry Research Experience

University of Washington Schlenker Lab **Seattle, WA**
Research Assistant, NSF Graduate Research Fellow *Winter 2016 - present*

- Projects involving perovskite solar cells and metal-free upconversion sensitizers
- Device fabrication and measurement
- Steady-state lock-in detected photoinduced absorption and photoluminescence

University of Rochester McCamant Lab **Rochester, NY**
Research Assistant *Spring 2015, Fall 2015-Spring 2016.*

- Solar Hydrogen Production project
- Qualitative studies of binding dyes to semiconductors (mainly TiO_2) through UV/Vis spectroscopy. Done to characterize the binding ability at different conditions

Senior Thesis

- Solar Hydrogen Production project
- Fluorescence quantum yield calculations of dyes through UV/Vis absorbance spectroscopy and emission spectra using a fluorometer. Study of the changes in fluorescence quantum yield when bound to various semiconductor materials.
- Synthesis of ceramic perovskite nanoparticles (strontium titanate) through hydrothermal autoclave method
- Calculation of theoretical resonance Raman spectra through use of quantum chemistry in the program ORCA

Rochester Institute of Technology Organic Photovoltaic Research Experience – Collison Lab **Rochester, NY**
Research Assistant *Summer 2015*

- Organic Photovoltaics REU
- Complete, on site fabrication of prototype bulk heterojunction OPV devices
- Photon-to-current efficiency testing of fabricated devices
- Characterization of thin films through UV/Vis absorbance spectroscopy and x-ray diffraction

Research experience resulted in contributing authorship of publication

Center for Enabling New Technologies Through Catalysis (CENTC) – Jones Lab **Rochester, NY**
Research Assistant *Summer 2014*

- Project focused on synthesis of a dicationic rhodium methyl aquo complex for use in catalysis to determine potential to functionalize methane to methanol
- Enhanced laboratory and research skills such as air and water sensitive synthesis, specifically using glove box and Schlenk techniques, and analysis of spectra

Professional Experience

DIRECT Trainee – Clean Energy Institute **Seattle, WA**
Data Intensive Research Enabling Clean Technologies, University of Washington *Fall 2020 – Spring 2021*

- Developed open-source Python-based software to model and visualize traffic changes in Seattle based on various input features
    - Project GitHub: https://github.com/Greening-Seattle

DIRECT Trainee – Clean Energy Institute, cont'd

- Developed open-source Python-based software to sort and visualize trends in Battery Management Software outputs for the King County Metro fleet of hybrid electric buses
    - https://github.com/KCM-DIRECT/KCM-Data
- Responsibilities included data cleaning, project management, geographic data segmenting and visualizations

Torrance Policy Analyst – Washington State Academy of Sciences **Seattle, WA**
In partnership with Clean Energy Institute, University of Washington *Summer 2020 – Spring 2021*

- Member of inaugural Policy Analyst cohort
- Authored whitepaper documents for the Washington State Academy of Sciences on topics such as decarbonization of Washington industries and equity in clean energy legislation

Graduate Research – University of Washington **Seattle, WA**
Research Assistant, NSF Graduate Research Fellow *Winter 2016 - present*

- Developed novel heavy-atom-free upconversion sensitizer platform
- Mastery in several techniques and instrumentations including:
    - Device fabrication and measurement
    - Steady-state lock-in detected photoinduced absorption and photoluminescence
- Mentoring and training experience with both junior graduate and undergraduate researchers.

Teaching Assistant – University of Washington **Seattle, WA**
Department of Chemistry, General Chemistry and Physical Chemistry *2016 – 2017, summer 2020*

- Led weekly labs, discussion sections, and office hours

Selected Employment and Campus Leadership Experience

- **President, Inclusion in Chemical Sciences, University of Washington** **2016-2020**
  Club activities involve educating and empowering women in science and their supporters by providing a safe and open space for dialogue, mentorship, collaboration, camaraderie, and skill building through a variety of activities including guest speakers and panels, student-facilitated discussions, workshops, and outreach to primary, secondary, and post-secondary institutions. Personal responsibilities involve maintaining the group website hosted on WordPress as well as planning and facilitating workshops, lectures, mentoring, and outreach events. Previously served as Webmaster, Vice President, and Outreach Coordinator.
- **Secretary, Chemistry Graduate Club, University of Washington** **2016-2019**
  Club activities include providing professional and social support to the graduate students in the Department of Chemistry at the University of Washington. Personal responsibilities involve maintaining the group website hosted on WordPress as well as planning and facilitating social events and visiting student weekends. Previously served as webmaster
- **Administrative Assistant, Department of Chemistry, University of Rochester.** **2013-2016**
  Employed as an administrative assistant to a staff member in the Chemistry department. Responsibilities include advertising and preparation for seminars, copying, outreach event planning, and various other administrative tasks.
- **Business Manager of the Undergraduate Chemistry Council** **2015-2016**
  Club activities include tutoring on campus and various outreach programs to encourage science education in the community. Personal responsibilities involved budgeting, purchasing, filing reimbursement forms, and general club maintenance.
- **Executive board member**
  "No Jackets Required" music appreciation/cover band organization **2015-2016**

  "Tiernan Project" Volunteering Organization/Living community **2013-2015**

Selected Outreach Activities

- **Henry M. Jackson High School Class Visit** February 15th, 2017
  Traveled to Jackson High School and made DSSCs using berry juice with an after school program
- **Night of Chemistry** April 14th, 2017
  Performed demos for 200+ people ranging from 2nd-11th grade (and parents)
- **Early Engineers** June 19th, 2018
  Guided a group of 20 students in making a solar panel from solar cells
- **Expand Your Horizons**
  March 19th, 2019
  EYH is a one-day STEM conference for girls in grades 8-12. Hosted 4 workshops, 35 minutes each, on astrochemistry/characterization.
- **WiSE Collective Pre Collegiate Summit** April 20th, 2019
  Demo table for an event that will target 9th-11th graders. It is intended to allow the students to get a glance at what pursuing a degree in science and engineering is really about.
- **Introduce a Girl to Renewable Energy** February 22th, 2020
  Guided a group of students in making rainbow bookmarks - a thin film of clear nail polish is used to create interference effects that create a rainbow on black paper

References

- Professor Cody Schlenker (206) 221-8627
  Assistant Professor, University of Washington, Department of Chemistry
- Yasmeen Hussain (206) 539-8559
  Program Officer, Washington State Academy of Sciences
- Professor Daniel Schwartz (206) 685-4815
  Professor, University of Washington
  Director, Clean Energy Institute
- Professor David McCamant (585) 276-3122
  Associate Professor, University of Rochester, Department of Chemistry
- Professor Christopher Collison (585) 475-6142
  Associate Professor, Rochester Institute of Technology, Department of Chemistry